Demonstrating load-change transient performance of a commercial-scale natural gas combined cycle power plant with post-combustion CO_2 capture

Corresponding author*: Rubén Mocholí Montañés

Address: Department of Energy and Process Engineering

NTNU – Norwegian University of Science and Technology

Kolbjørn Hejes vei 1b, Varmeteknisk * B347

NO – 7491 Trondheim, Norway

Phone: +47 735093722

e-mail address: ruben.m.montanes@ntnu.no

Demonstrating load-change transient performance of a commercial-scale natural gas combined cycle power plant with post-combustion CO_2 capture

Rubén M. Montañés[a*], Stefanía Ó. Garðarsdóttir[b], Fredrik Normann[b], Filip Johnsson[b], Lars O. Nord[a]

[a] Department of Energy and Process Engineering, NTNU - Norwegian University of Science and Technology, Trondheim, Norway

[b] Department of Energy and Environment, Chalmers University of Technology, Göteborg, Sweden

Abstract

The present work aims to study the transient performance of a commercial-scale natural gas combined cycle (NGCC) power plant with post-combustion CO_2 capture (PCC) system via linked dynamic process simulation models. The simulations represent real-like operation of the integrated plant during load change transient events with closed-loop controllers. The focus of the study was the dynamic interaction between the power plant and the PCC unit, and the performance evaluation of decentralized control structures. A 613 MW three-pressure reheat NGCC with PCC using aqueous MEA was designed, including PCC process scale-up. Detailed dynamic process models of the power plant and the post-combustion unit were developed, and their validity was deemed sufficient for the purpose of application.

Dynamic simulations of three gas turbine load-change ramp rates (2%/min, 5%/min and 10%/min) showed that the total stabilization times of the power plant's main process variables are shorter (10-30 min) than for the PCC unit (1-4 hours). A dynamic interaction between the NGCC and the PCC unit is found in the steam extraction to feed the reboiler duty of the PCC unit. The transient performance of five decentralized PCC plant control structures under load change was analyzed. When controlling the CO_2 capture rate, the power plant performs in a more efficient manner at steady-state part load; however, the PCC unit experiences longer stabilization times of the main process variables during load changes, compared with control structures without CO_2 capture rate being controlled. Control of L/G ratio of the absorber columns leads to similar part load steady-state performance and significantly faster stabilization times of the power plant and PCC unit's main process variables. It is concluded that adding the PCC unit to the NGCC does not significantly affect the practical load-following capability of the integrated plant in a day-ahead power market, but selection of a suitable control structure is required for efficient operation of the process under steady-state and transient conditions.

Keywords: Natural gas; Post-combustion; Control; Dynamic simulation; Operational flexibility.

1. Introduction

Atmospheric concentrations of CO_2 have increased by 40% relative to pre-industrial levels, primarily from fossil fuel emissions, and there is unequivocal base evidence that it is one of the major drivers of climate change [1, 2]. Limiting climate change would require maintained and substantial reductions of anthropogenic greenhouse gas (GHG) emissions during the next decades and near zero GHG emissions by the end of the 21st century [2]. Nevertheless, it is expected that coal and natural gas will remain as important energy sources for electricity generation in long-term global prospects to 2040 [3]. Implementation of carbon capture and storage technologies (CCS) can significantly reduce the life cycle CO_2 emissions of fossil fuel power plants [4].

Natural gas combined cycle power plants have moderate capital costs, short construction times and high efficiency and flexibility [5, 6]. State-of-the art large-scale natural gas combined cycle (NGCC) power plants with three-pressure reheat configurations (3PRH) have recently reached lower heating value (LHV) fuel efficiencies of above 60% by different vendors [7]. This LHV fuel efficiency is higher than most efficient coal-based power plants with up to 47% LHV fuel efficiency. In addition, at 350-450 $kgCO_2/MWh$, combined cycle power plants are less carbon intense than their coal-based counterparts at

750-1000 kgCO_2/MWh [8]. These facts might drive the implementation of combined cycle natural gas-fueled power plants in the transition towards future low-carbon energy systems in different areas of the world. As concluded in [9], conventional NGCC power plants are likely to be serious competitors to coal with CCS in the short to medium term. According to the International Energy Agency, the global average carbon intensity of power plants being operated today is around 530 kgCO_2/MWh, which is still far away from the 100 kg/MWh global average required in the power sector to be consistent with a 2°C climate scenario by 2050 [8]. Therefore, in the medium to long term, CCS might be required to enable the reduction of CO_2 emissions from NGCCs by retrofitting existing units and extending their lifetime or by implementing novel advanced process configuration concepts with higher levels of process integration.

The most promising near-term technology to implement post-combustion CO_2 capture from combined cycle power plants is that of chemical absorption with solvents [10]. NGCC power plants with PCC can reach carbon intensities of below 50 kg/MWh [11]. Chemical absorption with 30%wt aqueous monoethanolamine (MEA) is commonly used as the benchmark solvent for most of the academic work related to integrated studies of NGCC power plants with post-combustion CO_2 capture based on process simulation.

The increasing share of variable renewable energy sources in electricity generation changes the operating role of base load thermal power generating units [12, 13]. NGCC power plants will be operated as load-following, with an increased number of start-ups and shutdowns, and providing fast cycling capabilities [14]. That includes thermal power plants with CCS [6, 15]. The Carbon Capture and Storage update 2014 concludes that the financial case for CCS requires that it operates in a flexible manner, and load-following ability is considered extremely important for the long-term economics [16].

A key aspect of the operational flexibility of power plants with post-combustion CO_2 capture using amines is the steady-state design and part-load off-design performance of the power plant. Recent simulation studies have analyzed the part-load performance of the NGCC plant integrated with post-combustion CO_2 capture for different process configurations and process integration concepts [17]. These concepts include exhaust gas recycle (EGR), partial reboiler integration in the heat recovery steam generator (HRSG) and the eco-reboiler concept [18]. A previous work [17] suggested that understanding the dynamic interaction between the power plant and the PCC unit remains a key aspect for developing the NGCC PCC technology. In addition, it was concluded in [11] that a key area of future work should be the inclusion of detailed dynamic process models of the power plant when analyzing the transient performance of the PCC plant integrated with post-combustion CO_2 capture.

The transient or time-dependent behavior of the chemical absorption PCC process is characterized by being relatively slow, compared to that of the combined cycle power plant. Despite the increased interest in carrying out transient test campaigns in pilot chemical absorption plants to assess the transient performance and operational flexibility of the chemical absorption process with MEA [17] [19], most of the work to assess transient plant performance and control has been based on dynamic process simulation [20]. Recent work by [21] carried out open-loop step responses on the plant via dynamic process simulation of validated models, where they characterized the transient response of several process variables (outputs) to step changes in main inputs to the plant, concluding that one can expect long dead times and relatively large settling times – in the order of hours.

A key area of research within the dynamic operation of the PCC process is the development and analysis of plant-wide control strategies for the post-combustion capture process [22] [23] [24] [25]. Most of the published work focuses on flue gas from a coal-based power plant [20]. In these analyses the flue gas is considered a disturbance to the process, and the steam coming from the power plant to feed the reboiler duty required to regenerate the solvent is considered as a boundary condition, omitting dynamic interactions between the power plant and the post-combustion capture unit. A recent report from the IEAGHG includes a literature review and assessment of control strategies for the PCC process [15]. It

concludes and recommends that future work should include detailed dynamic process models of the power plant with advanced dynamic process modeling tools. Some studies have assessed simulation of the NGCC process with post-combustion CO_2 capture, however these works do not implement detailed dynamic process models and controllers of the power plant [26, 27]. He and Ricardez-Sandoval mention to have included a dynamic process model of the power plant in Aspen Plus® for analysis of the integrated process, but details on the dynamic process model of the power plant were not presented, and it is stated that to simplify their analysis, the off-design dynamic performance evaluation of the gas turbine and steam turbine under transient operations were not included. Their work concludes that future work in this research should aim at developing suitable control strategies for the integrated system and to study the dynamic operability of the closed-loop under changes in the power plant.

Due to the lack of operational experience of the commercial-scale integrated NGCC power plant with PCC, there is a need to assess its load-following capability via dynamic process simulation. Previous plant-wide control studies found in literature omitted the dynamic interactions between the power plant and the PCC systems. The aim of this work is to assess the transient performance of the NGCC with PCC during load changes, in order to gain understanding of the dynamic interaction between the power plant and the PCC unit. The study includes the identification and evaluation of suitable decentralized control structures for the integrated process. Firstly, we describe the power plant process configuration and design procedure, including PCC process scale-up. Secondly, the process models of the gas turbine (GT), steam cycle and PCC system are described, with an emphasis on the detailed dynamic process models of the steam cycle. The validation of the dynamic process models is assessed. Then, the performances of different control strategies for both the power plant and the PCC plant are discussed. Finally, we demonstrate and explain the transient load change of the NGCC with PCC and assess the performance of different decentralized control structures for the integrated process.

2. Power plant description

2.1. Natural gas combined cycle power plant configuration

The NGCC power plant consisting of a 3PRH HRSG was designed by means of the process simulation software, Thermoflow [28]. As shown in Figure 1, the NGCC has been designed considering the heat integration with the PCC plant. Steam extraction from the intermediate pressure (IP) and low pressure (LP) turbine crossover and steam from the LP superheater are mixed, de-superheated, and sent to the reboiler in order to feed the reboiler duty of the PCC system. The utilization of Thermoflow [28] allows detailed design data including main plant components' geometry, materials and process flowsheet to be obtained. In addition, it provides reliable steady-state full-load and part-load performance data of the plant, for both GT and steam cycle. These data reflect the current technology performance of the power plant and have been considered as a reliable source of plant performance under off-design loads in the literature [17]. Therefore, the performance data for off-design loads was used in this work as a reference for steady-state design and off-design validation of the dynamic process models of the combined cycle power plant configuration. In addition, detailed geometry, flowsheet and materials are required as inputs to parameterize the main dynamic process models of the steam cycle.

The key performance data at design load of the natural gas combined cycle power plant NGCC-PCC are shown in Table 1 including main steam cycle parameters. Fuel is assumed to be 100% CH_4, and the GT has a dry low NO_x combustor. The flue gas flow to the capture plant is assumed to be free of flue gas components SO_2 and NO_x.

2.2. Post-combustion CO_2 capture unit configuration

A post-combustion capture unit with 30% wt MEA as chemical solvent was designed with the commercial software, Aspen Plus® [29]. The process configuration considered was the one with two absorbers and one stripper, as proposed by Jordal et al. [17], following the methodology presented in

[30]. Modified process configurations, including absorber inter-cooling, solvent split flow or lean vapor recompression stripping, as studied by Amrollahi et al. [31], were not considered in this paper. Therefore, no attempt was made to optimize the plant's steady-state performance.

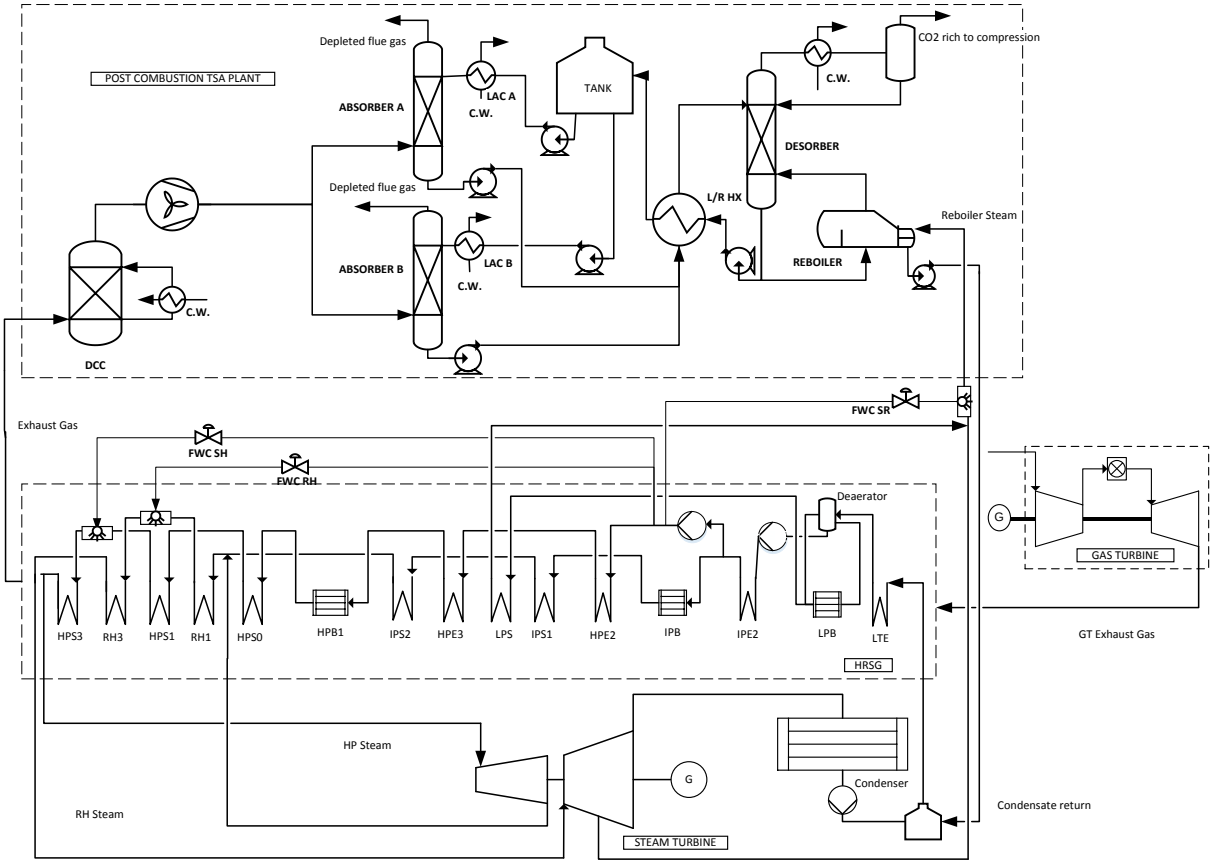

Figure 1. Process flow diagram of the NGCC power plant integrated with post-combustion CO_2 capture.

Table 1. NGCC with PCC performance data summary.

Gas Turbine	Mitsubishi 701 JAC
GT Power Output [MW]	451.8
Fuel	CH_4
Fuel lower heating value [MJ/kg]	50.047
GT Exhaust mass flow [kg/s]	887.1
GT Exhaust temperature [^{0}C]	632
HRSG efficiency [%]	82.81
Steam turbine gross power [MW]	161.1
Plant net LHV electrical efficiency [%]	52.38 %
HP pressure and temperature [bar/^{0}C]	145/591
RH pressure and temperature [bar/^{0}C]	30/591
LP pressure and temperature [bar/^{0}C]	3.69/290
Crossover pressure [bar]	3.69
Condenser pressure and temperature [bar/^{0}C]	0.0483/32.25
Cooling water temperature [^{0}C]	15
HP/IP/LP dry section efficiencies [%]	87.9/92.3/93.8
HP turbine inlet flow [kg/s]	111.15
IP turbine inlet flow [kg/s]	125.7
LP steam generated in HRSG [kg/s]	12.9
LP turbine extraction flow [kg/s]	3.7

The design point chosen for the post-combustion unit is 100% GT load under ISO conditions, which, for the Mitsubishi 701 JAC gas turbine, corresponds to flue gas with mass flow rate of 887.1 kg/s with

4.33 vol % CO_2 (wet). The design target CO_2 capture rate is 90% at 100% load operation. The flue gas from the HRSG is cooled from 126 ^{0}C down to 40 ^{0}C with a direct contact cooler (DCC) and fed to both absorbers (443.55 kg/s of flue gas per absorber at design conditions). Mellapack 350Y structured packing was selected for the absorbers and stripper. The diameter of the absorber columns was determined by setting 65% flooding limit for absorbers and 70% for stripper column, to be consistent with previous work in [17]. Relevant input data for the simulations and scale-up of the PCC unit are shown in Table 2. Table 3 shows a list with main residence times and solvent hold-ups at design points in different parts of the PCC system. Residence times have been chosen according to data published in the literature [32].

Table 2. Absorber columns, heat exchanger and desorber design data [17] [33].

Absorber columns	
Diameter [m]	16.3
Height [m]	23.2
Packing material	Mellapak 350Y
Design flooding limit [%] **[17]**	0.65
Lean loading	0.27
Rich loading	0.5
Whole column pressure drop [bar]	0.06
Inlet gas velocity [m/s]	1.9
Pressure at top of column [bar]	1.1
Lean solvent inlet temperature [degC]	40
Stripper	
Diameter [m]	9.7
Height [m]	10
Packing Material	Mellapak 350Y
Pressure at top of column [bar]	2
Whole column pressure drop [bar]	0.06
Design flooding limit [%] **[17]**	0.7
Heat Exchanger	
Average U-value [W/m^2·K] **[33]**	2000
Lean-rich temperature approach [K]	5
Heat exchanger area [m^2]	27855.3

Table 3. Residence time, volumetric flow and solvent hold-up at different parts of the PCC system, based on data from literature [32].

	Residence time [min]	Volumetric flow solvent [m^3/min]	Hold-up [m^3]
Absorber sump	5	32.9	164.6
Buffer tank	16	68.8	1100.5
Reboiler	5		353.2
Desorber sump	5	70.7	353.3
Desorber sump and reboiler	10	70.7	706.6
Cross heat exchanger and piping	26	66.8	1736.7
Reboiler steam side	1	5.9	5.9

2.3 Process integration

Two key integration aspects for this specific configuration of a NGCC-PCC plant are the exhaust gas from the HRSG stack sent to the chemical plant and the steam extraction from the steam turbine to feed

the reboiler. Since CO_2 is captured from the GT exhaust gas, pressure drop will be imposed in the flue gas line by the HRSG recuperators and bypass-stack system with dampers, the DCC, the absorber column packing and washer sections, and additional ducts and stacks. Most of this pressure drop is overcome by the GT. From an efficiency point of view, it is advantageous to let a fan, rather than the gas turbine, overcome this pressure drop. Therefore, a fan was included in the flue gas line after the DCC cooler to overcome the additional pressure drop imposed mainly by the absorber column.

A second important thermodynamic interface between the PCC process and the power plant is the steam extraction from the steam turbine to provide the heat required for solvent regeneration and to generate the stripping vapors flowing upwards through the stripper column. This integration aspect has been widely discussed in literature for both gas and coal-fired power plants with post-combustion CO_2 capture [34-37]. The most efficient method of providing that heat is to condense the steam extracted from the power plant. Due to solvent degradation problems, the temperature of the solvent in the reboiler should be limited within the range of 120 – 122 ^{0}C. Therefore, the supply temperature of the steam should at least be 130 ^{0}C at saturation, when considering a differential temperature approach to be at least 10 ^{0}C. This corresponds to a steam pressure of 2.7 bar. In addition, the process conditions for steam supply to the reboiler should be above these to overcome the piping pressure losses. In this work the integration methodology with steam extraction from the IP/LP crossover has been applied as presented in [36]. The IP/LP crossover extraction option for reboiler heat integration has also been implemented in previous part-load performance studies for 3PRH power plant with post-combustion CO_2 capture with aqueous MEA as solvent [38]. Steam extracted from the IP/LP crossover at 3.7 bar is mixed with steam from the LP superheater. The steam is de-superheated by water injection from the high pressure (HP) feedwater line of the HRSG (refer to FWC SR in Figure 1). The HP water extraction is regulated by a throttling valve, with the objective of controlling the steam temperature of the superheated steam sent to the reboiler at 150 ^{0}C, with the purpose of preventing solvent degradation. Under design conditions, steam extracted from the IP/LP crossover, from the LP superheater and from the HP water extraction, represents, respectively, around 71%, 14%, and 15% of the total steam fed to the reboiler. Sufficient steam must be available at the extraction for solvent regeneration under part-load operation [17]. Steady-state off-design simulations conducted during this work revealed that enough steam is available at the extraction for part loads down to 60% GT load. The condensate from the reboiler is sent to a feedwater tank, where it is mixed with the feedwater coming from the steam turbine condenser. All feedwater is circulated to the low temperature economizer in the HRSG (refer to Figure 1).

Extracting steam from the steam turbine results in lower steam flow rate through the LP turbine and condenser and, hence, reduced turbine power output. The LP steam turbine has been sized for operation with the post-combustion system operating under full-load plant operation. This results in a smaller LP turbine, condenser and generator than if the LP turbine is designed for temporary CO_2 capture shutdown. Thern et al. [35] discuss implications of temporary CO_2 capture shutdown for LP steam turbine design and performance. A recent study [38] discusses the impacts of non-capture operation on IP and LP turbine efficiency and condenser backpressure; it concludes that, if the NGCC plant is to be operated with an integrated post-combustion CO_2 capture scheme, it is not beneficial to operate it in a standalone mode (non-CO_2 capture operation), aside from inevitable situations such as CO_2 capture plant or compression train unit trip.

3. Dynamic process model description for power plant and post-combustion plant

3.1. Dynamic process models of the power plant

The dynamic process models in this work were developed with the open physical modeling language, Modelica[39]. The dynamic process models implemented in Modelica were obtained from the ThermalPower library (TPL) [40]. The base models were utilized to build up the power plant model as designed in Thermoflow [28], by using the dynamic process-modeling environment, Dymola [41]. Accumulation of energy and mass within process equipment is highly dependent on fluid inventories and equipment size. Therefore, dynamic process models from the ThermalPower library require design data of the equipment for model parameterization, obtained from Thermoflow [28]. Those data include

equipment size, tube geometry, hold-up of vessels and residence times, wall materials, fluids' property packages, drum geometry and wall thickness.

3.1.1. Gas turbine model

It is a generalized approach in load-change transient modeling and simulation of combined cycles to omit the full dynamic process model of the GT [42, 43]. For transient applications, the GT is normally modeled with the block diagram approach to simulate its governor controls [44] [45]. In this work, a quasi-static approach is considered, in which the off-design performance of the GT exhaust's temperature and mass flow rate is implemented. Small variations in exhaust gas composition were disregarded, since those were found to be small for the operating window studied in this work. A common procedure is to simulate the steady-state off-design performance of the GT and include the key characteristics of the exhaust as a disturbance to the dynamic process model of the HRSG and turbine island. By assuming a ramp rate, a turbine exhaust time series can be tailor-made to simulate the GT load change; refer to Figure 2. This method is justified because of the faster transient performance of the GT than that of the steam cycle due to the HRSG thermal inertia [45]. Hence, the GT exhaust characteristics for different loads were modeled as a disturbance to the HRSG gas-side process models. The exhaust gas from the gas turbine, consisting of a mixture of Ar, H_2O, O_2, N_2 and CO_2, is modeled with the ideal thermodynamic equation of state, and thermochemical properties are calculated using a seven-coefficient version of the NASA ideal gas properties.

A steady-state model in Thermoflow [28] was used to obtain the validated part-load performance of this GT. Table 4 shows the main performance values of the GT at loads from 100% to 60%, for ISO ambient conditions. Figure 2 includes the steady-state off-design loads' gas turbine characteristics in terms of exhaust temperature, mass flow rate and gross power. Figure 3 shows the time-dependent exhaust temperature and mass flow for an event with load reduction from 100% GT load to 80% GT load, with a typical GT load reduction of 5%/min [14]. Load change rate from one load point to another would be typically 4-5% per min, for both load increase and load decrease, for a combined cycle [14, 17].

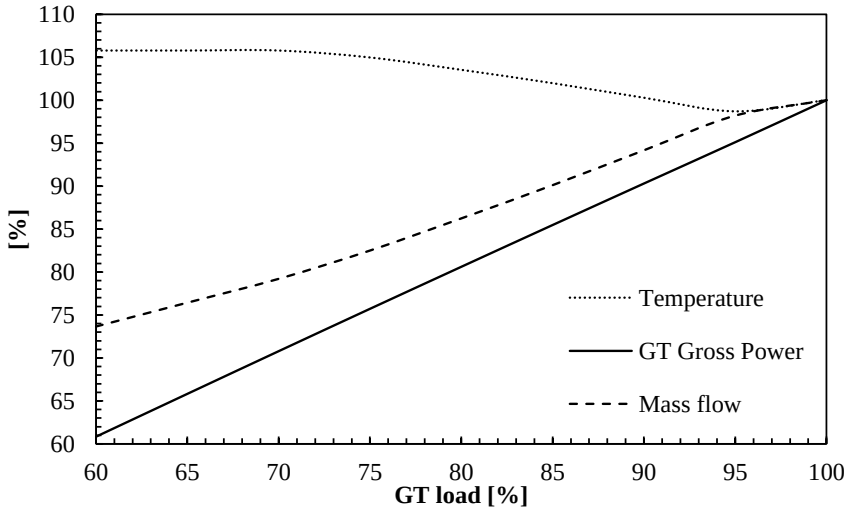

Figure 2. GT exhaust characteristics at different steady-state off-design loads with ISO ambient conditions.

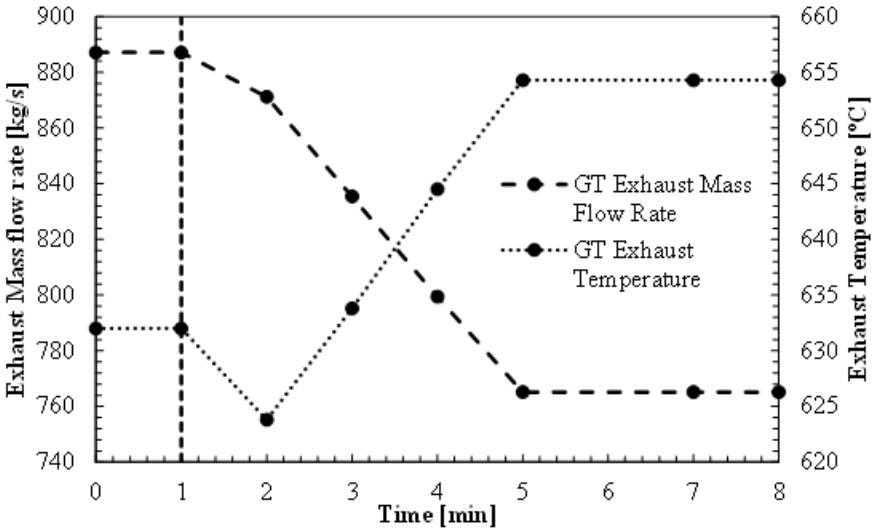

Figure 3. Time-dependent tailor-made GT exhaust characteristic considering a quasi-static modeling approach. GT load reduction from 100% to 80% load. Transience starts at minute one.

Table 4. Main performance values of the Mitsubishi 701 JAC for ISO ambient conditions, at different off-design loads.

GT Load %	**100**	**95**	**90**	**85**	**80**	**75**	**70**
GT gross power [MW]	451.8	429.7	407.9	386.1	364.2	342.1	319.8
GT fuel LHV chemical energy input (77F/25°C) [MW]	1081.5	1038.7	1002.1	965.2	927.5	889.1	849.2
Turbine exhaust mass flow [kg/s]	887.1	871.2	835.4	799.4	765.1	731.9	702.7
Turbine exhaust temperature [C]	632	623.8	633.8	644.5	654.3	663.4	668.5
Exhaust gas N_2 mole fraction [%]	73.97	74.04	74.02	74	73.99	73.98	74
Exhaust gas O_2 mole fraction [%]	11.25	11.46	11.4	11.34	11.3	11.28	11.33
Exhaust gas CO_2 mole fraction [%]	4.33	4.23	4.26	4.29	4.30	4.31	4.29
Exhaust gas H_2O mole fraction [%]	9.56	9.38	9.43	9.48	9.52	9.53	9.49
Exhaust gas Ar mole fraction [%]	0.89	0.89	0.89	0.89	0.89	0.89	0.89

3.1.2. Heat recovery steam generator, deaerator and condenser models

The heat recovery steam generator of this plant consists of horizontal three-pressure levels with reheat system. It has three drum systems with evaporator (LPB, IPB, HPB), including an integrated LP drum and deaerator system (LPB and DA). In addition, there are a total of 12 finned tube flue gas to water and steam recuperators. The recuperators consist of four economizers (LTE, IPE2, HPE2 and HPE3), six superheaters (LPS, IPS1, IPS2, HPS0, HPS1 and HPS3) and two reheaters (RH1 and RH3). Two inter-stage superheated steam temperature control systems are implemented: one between the last two superheaters and the other between the two reheaters. Such systems use high pressure water from the HP feedwater line upstream of the high pressure economizer, HPE2. The HP water is injected into the pipe between the superheating and reheating stages, and consequently the temperature is reduced by evaporative cooling. A valve implemented for the extraction is manipulated to change the HP water mass flow rate and hence control the temperature of the steam sent to HP and IP steam turbine intakes. The water and steam thermophysical property package is implemented by using the IAPWS-IF97 standard, with analytic derivatives [46].

The heat exchanger recuperator model is built from base physical process components of hot side piping, conductive heat transfer wall and cold side piping. Both pipes and wall are discretized in the axial direction, and heat transfer equations are solved in a discretized manner. The process model

configuration assumes counter-current flow, while the physical configuration is cross-flow. Note that, in a HRSG heat exchanger the entire metal mass has a specific geometry with bare tubes with serrated fins on them. As discussed in [43], for transient simulations, an important consideration is the wall temperature evolution over time. A typical approach is to consider the whole heat exchanger metal mass as a lumped metal cylinder, since in the exhaust flow gas path the tubes are quite close to each other and have a high density of fins; thus, the entire heat exchanger is substituted by a lumped cylinder with the same mass (volume and density) and external heat transfer surface area as the real heat exchanger (HX) [45]. The cylinder has a wall thickness equivalent to that of a single tube and geometry (length and diameter) and is calculated so as to consider the overall heat transfer area and metal mass as the actual heat exchanger. Therefore, the hypothetical heat exchanger model is a 1-D counter-current model, which is then discretized in the axial direction in *n* volumes.

The dynamic discretized pipe models are implemented with a similar modeling approach for both gas and water/steam side. For the gas side, mass, mass fraction and energy balance equations are discretized by means of the finite volume method, with *n* the number of volume segments. For this work, static balances on the gas side have been considered, since such processes are relatively fast [42]. A uniform velocity is assumed in the cross-section leading to a 1-D distributed parameter model. The state variables are mass fractions, *n* temperatures and a lumped pressure. The energy balance equation is written by assuming a uniform pressure distribution, and the pressure drop calculation is lumped at the piping outlet. Longitudinal heat transfer diffusion is neglected within the pipe.

For the water/steam side, the model allows for calculation of both fluid states with one-phase or two-phase mixture, and it uses the integrated mean density and lumped pressure approach. The model consists of dynamic mass and energy balances with static momentum balance; equations are discretized as well by means of the finite volume method, with *n* the number of volume segments.

Fluid flows in the pipes can exchange thermal power through the lateral heat surfaces, which are connected to the wall process model. This allows the calculation of convective heat transfer between the water/steam fluid bulk and the wall's inner surface, and between the gas bulk and the wall's outer surface. A wall model for transient conductive heat transfer, considering the capacity of the metal to store heat (thermal inertia) and the resistance for conductive heat transfer, is implemented in the HX model. The wall is discretized in *n* segments in the longitudinal direction. Longitudinal wall conductive heat transfer is neglected. For this application, a discretization of the wall model in the radial direction was not considered, but it would be possible to do so for thermal stress estimation applications, as presented by Benato et al. [47].

The convective heat transfer coefficient for 1-phase gas flow over tube bundles is modeled continuously with a Nusselt correlation covering the entire flow region, and the flow is considered to be thermally and hydraulically developed. The heat transfer coefficient h_g is computed for each segment as in Equation (1), where F_a is a tube arrangement factor, λ is the thermal conductivity of the gas and d_{hyd} is the hydraulic diameter of the pipe. The Nusselt number for each row is calculated by Reynolds-dependent correlations from [48].

$$h_g = \frac{F_a Nu_0 \lambda}{d_{hyd}} \tag{1}$$

For the water side, a heat transfer correlation has been considered for estimating the convective heat transfer coefficient for superheaters, h_s, for 1-phase; see Equation (2). A similar formulation is employed for economizers. The mean Nusselt number, Nu_m, is calculated by Reynolds-number-dependent correlations from [48].

$$h_s = \frac{Nu_m \lambda}{d_{hyd}} \quad (2)$$

For the two-phase flow in the evaporators, a constant heat transfer coefficient of 120 kW/m^{2}K for the cold side was considered. The pressure drop in both the cold and hot sides is computed with Colebrook's equation, where the hydraulic friction coefficient *f* is specified by the nominal operating point (mass flow rate, pressure drop and density).

The main function of a drum in a subcritical HRSG is to separate the steam from the liquid water, at a given pressure level. Transient phenomena and dynamic modeling of drum boilers has been studied extensively [49]. As described in [50], one difficulty in power plant control is the drum-level control problem, due to the known shrink and swell effect. The drum model available in the ThermalPower library is capable of capturing pressure and drum-level dynamics and includes wall dynamics. The model describes the cylindrical drum of a drum boiler, where there is no thermodynamic equilibrium between the liquid and gas hold-ups. The drum and evaporator dynamic process model included in TPL [40] uses the formulation described in [51]. The required parameterization of the model is mainly the equipment data (geometry and material properties). Natural circulation in the drum-evaporator system was implemented by means of an ideal height difference model with pressure head for modeling the downcomers and risers of the system.

In a steam power plant, the main function of the deaerator is the removal of non-condensable gases such as CO_2 and O_2. The objective is to avoid synergetic corrosion effects within the water tubes of the HRSG, which would reduce the lifetime of the plant considerably [52]. In this case, the deaerator model is simulated to consider the water/steam inventory under transient conditions. Therefore, the medium in the process model is water/steam. The dynamic process model assumes thermodynamic equilibrium between the liquid and vapor hold-ups (same temperature and pressure), and takes into account variable hold-ups (level and pressure must be controlled).

The condenser model is a model of a cylindrical condenser that assumes thermodynamic equilibrium between vapor and liquid hold-ups. In addition, a dynamic wall model accounting for transient wall effects is included in the model. The wall separates the condensing steam from the cooling media. The wall model considers the capacity of the tubes to store heat under transient conditions. The cooling liquid heat transfer uses a liquid correlation, valid for both laminar and turbulent flow. It uses a logarithmic average of the cooling inlet and cooling outlet temperatures as the driving temperature. A correlation for heat transfer condensation over tube bundles has been implemented for the water/steam side of the condenser [48]. The model includes a hotwell that collects the liquid hold-up. The level of water in the hotwell has been decided by considering the design inventory of water in the condenser, as defined in Thermoflow [28]. The cooling water inlet temperature and the mass-flow under part-load conditions are maintained as constant.

3.1.3. Steam turbine models

For the range of part-load operation considered in this study (100-60% GT load), the steam cycle of the combined cycle plant is operated under sliding pressure operation mode [53]. The steam turbine model is assumed as a quasi-static model. This is justified because the purpose of the transient model is to simulate the load-following transient event; therefore, the main thermal inertia of the system consists of the HRSG inertia [43]. Effects of steam turbine rotor dynamics and steam turbine casing and rotor thermal inertia are not of interest here, since those are normally relatively fast. Therefore, dynamic interactions between the power grid and the steam cycle in terms of real-time frequency control-related transients are neglected, as those are outside the scope of this work. Steam turbine expansion is defined by the swallowing capacity and the isentropic efficiency. Stodola's law of cones is used to define the swallowing capacity of the turbine (Equations 3-4), where K_t is the flow area coefficient, based on the nominal flow conditions of pressure and density, subscript *n* stands for nominal conditions, *i* for inlet, *o* for outlet, and F_t for mass flow through the turbine.

$$K_t = \frac{\dot{F}_n}{\sqrt{p_{i,n} \cdot \rho_{i,n} \cdot \left(1 - \left(\frac{p_{o,n}}{p_{i,n}}\right)^2\right)}} \quad (3)$$

$$\dot{F}_t = K_t \cdot \sqrt{p_i \cdot \rho_i \cdot \left(1 - \left(\frac{p_o}{p_i}\right)^2\right)} \quad (4)$$

Turbine expansion was assumed to have constant isentropic efficiency under variable loads. For different loads, the steam turbine has approximately constant volumetric flow. This helps to keep the velocity triangles of the stages approximately constant, and therefore the efficiency remains approximately unchanged [52]. Dry isentropic efficiencies were assumed to be 0.88, 0.923, and 0.931, for the HP, IP and LP sections, respectively. In addition, the efficiency of the LP section of the steam turbine has been corrected for the moisture content, since the expansion crosses the Wilson line [52]. The dry efficiency degradation is a function of the steam quality and can be expressed by Bauman's formula, Equation (5). The Bauman's coefficient K_b has been set to 0.8 [52]. A simplified generator model is included to account for mechanical shaft and generator losses, with a constant mechanical efficiency of 0.98.

$$\eta_{is} = \eta_{is,dry} \cdot \left(1 - K_b \cdot (1 - x_{mean})\right) \quad (5)$$

3.2. Dynamic process model of the post-combustion CO_2 capture plant

The dynamic process models for the main equipment of the PCC plant are implemented in the Modelica language. A library called Gas Liquid Contactors [54], containing dynamic process models of the main equipment of the PCC unit, has been utilized as a basis for this work. For a detailed description of the models and equations, the reader should refer to [55] and [56]. The Modelica models were calibrated to fit the design point data from the AspenPlus® design of the two-absorber and one-desorber scaled-up plant, as described in Table 2. Calibration included matching temperature profiles of the absorber and desorber columns, lean/rich loadings at the inlet and outlet of columns and absorption and desorption rates. The main calibration factor was the enhancement factor for chemical reactions.

4. Process model validation

The power plant dynamic process model has been validated against steady-state data for both design and off-design conditions by comparing the results obtained from Thermoflow [28]. Absolute percentage errors *AP* in Table 5 are calculated based on Equation (6), while mean absolute percentage errors *MAP* are based on Equation (7), where R_t is the reference value and S_t is the value from simulations.

$$AP = 100 \left|\frac{R_t - S_t}{R_t}\right| \quad (6)$$

$$MAP = \frac{100}{n} \sum_{t=1}^{n} \left|\frac{R_t - S_t}{R_t}\right| \quad (7)$$

The gas side HRSG's temperature profile under design conditions was validated, and mean absolute error was found to be 0.16 %, maximum absolute error being 0.62% (not shown). Table 5 includes validation results of the steam turbine gross power, HP and RH steam admission pressures for different GT loads.

The transient performance in terms of steam turbine power output showed correct behavior in respect of 99% settling time for load changes with a 5%/min GT load ramp rate. Note that, by settling time, we mean here the time required for the response curve to reach and stay within a range of 1% of the final value. These settling times were similar to those reported in Thermoflow software [28]. In addition, a similar modeling methodology for predicting transient performance of NGCCs has been utilized in literature [47], resulting in similar settling times of 6-9 minutes. This means that the dynamic process model of the power plant is also capable of capturing the process dynamics with high fidelity. Therefore,

it can be concluded that the power plant dynamic process model is capable of predicting proper steady-state performance under different loads to an appropriate level of accuracy, required for the analysis, and predicts transient trends under load change transient event driven by the GT load reduction.

Table 5. Validation of the power plant model under off-design GT load operation.

	ST gross power [MW]			HP admission pressure [bar]			RH admission pressure [bar]		
GT Load	**GT pro**	**Dymola**	**Error %**	**GT pro**	**Dymola**	**Error %**	**GT pro**	**Dymola**	**Error %**
100	161091	161444	0.22	145	145.3	0.20	30	30.4	1.23
95	154716	154767	0.03	139.2	139.9	0.55	28.9	29.2	0.98
90	153359	153260	0.06	137.3	137.3	0.02	28.5	28.8	1.11
85	151046	151020	0.02	133.8	133.6	0.17	28.2	28.5	1.08
80	148347	148373	0.02	130.2	129.7	0.37	27.8	28.2	1.19
75	145356	145343	0.01	126.5	125.8	0.58	27.3	27.6	0.99
70	141617	141501	0.08	122.5	121.6	0.74	26.6	26.9	0.96
MAP			0.06			0.38			1.08

The models of the post-combustion capture plant were validated in a recent work by Montañés et al. [57]. That work uses large-scale steady-state and transient data from an amine pilot plant with flue gas from a natural gas-fired power plant at CO_2 Technology Centre Mongstad [58].

5. Proposal of different control structures

The day-to-day operation of thermal plants can be handled by closed-loop control [53]. The main objective of the control system is to provide load control and frequency response. Frequency response is utilized when sudden increases or decreases in electrical power load are required [59] and is normally provided by the gas turbine and by the steam turbine if it is designed to do so. The load of the combined cycle is controlled by means of the GT load reduction/increase. The steam cycle will follow the GT load change by providing power with the available steam generated in the HRSG. Once a GT load change is applied, the steam turbine load will adjust automatically with a time delay of about 10-15 minutes [53], normally defined by the thermal inertia added by the HRSG. In this regard, the GT load change can be seen as a disturbance to the steam cycle. In addition, from the PCC plant's perspective, the exhaust gas coming from the NGCC power plant is a disturbance to the process; thus, the control system of the PCC plant must be capable of handling this disturbance under load changes.

The control system of a process plant is typically designed in a hierarchical manner, with different tasks assigned to different control layers. As described in the literature [53, 60], the control layer of a chemical and a power plant can be divided into two main layers: the regulatory control layer ("base control") and the supervisory control layer ("advanced control").

- Regulatory control layer: The main task of the regulatory control layer is to stabilize the plant's drifting variables under fast disturbances and keep these variables close to the set-points in the fast timescale. Stabilization here means that the process does not drift away from acceptable operating conditions under disturbances. This normally implies controlling temperatures, pressures and levels, and having a consistent inventory control structure [61].

- Supervisory control layer: The supervisory control layer is used to control variables that are more important from an overall point of view, i.e., in a longer timescale. It is the slower upper layer that acts on the set-points of the regulatory control layer or remaining degrees of freedom. This layer will be in charge of supervising load changes.

In the following, the control structures implemented in the dynamic process models are presented. Functions related to logic on start-up/shut-down and safety systems of the plant were not included in this work.

5.1. Control layers for combined cycle

The gas turbine in a combined cycle is normally provided with a standardized control system and therefore the gas turbine supplier provides an engine that is already automatized for operation. The gas turbine load is controlled by the combination of variable inlet guide vanes (VIGVs) and fuel mass flow rate [53]. VIGVs allow modification of the air mass flow rate input to the gas turbine. The main objective during part-load operation is to keep high turbine inlet temperatures (TIT) and turbine exhaust temperatures (TET) under part loads, since that will allow highly efficient part-load operation of the steam cycle. TIT is normally controlled by a combination of fuel flow input and the position of the VIGVs; this keeps high levels of both TIT and exhaust gas temperature at part loads. In modern gas turbines, this strategy can be utilized down to about 40% GT load, from which the VIGVs' saturate and air mass flow rate cannot be further reduced. Lower loads can be achieved by further reducing fuel input flow rate, but the TIT cannot be kept at high values. In this work the GT model is a quasi-static model. To control the steam production in the HRSG at part loads, a strategy called sliding pressure operation is normally implemented. With sliding pressure operation mode, the steam turbine inlet control valves are fully open, so that the admittance pressure is sliding or floating. This allows high levels of efficiency to be maintained in the steam cycle, compared with strategies in which the HRSG steam pressures are controlled by valve throttling, partial arc admission or hybrid configurations [62]. Sliding pressure operation is normally applied down to approximately 50% live-steam pressure, from which a control strategy based on pressure control via valve throttling is applied [53]. Valve throttling will be required under normal operation to provide a fast frequency response, if the steam cycle is designed to do so.

Figure 4 shows the regulatory control layer implemented in the steam cycle. It includes the essential control loops that are required in order to ensure stable steam cycle operating conditions in the combined cycle power plant under stable operation and for load changes driven by GT load changes. The controllers were implemented in the dynamic process models and are described as follows:

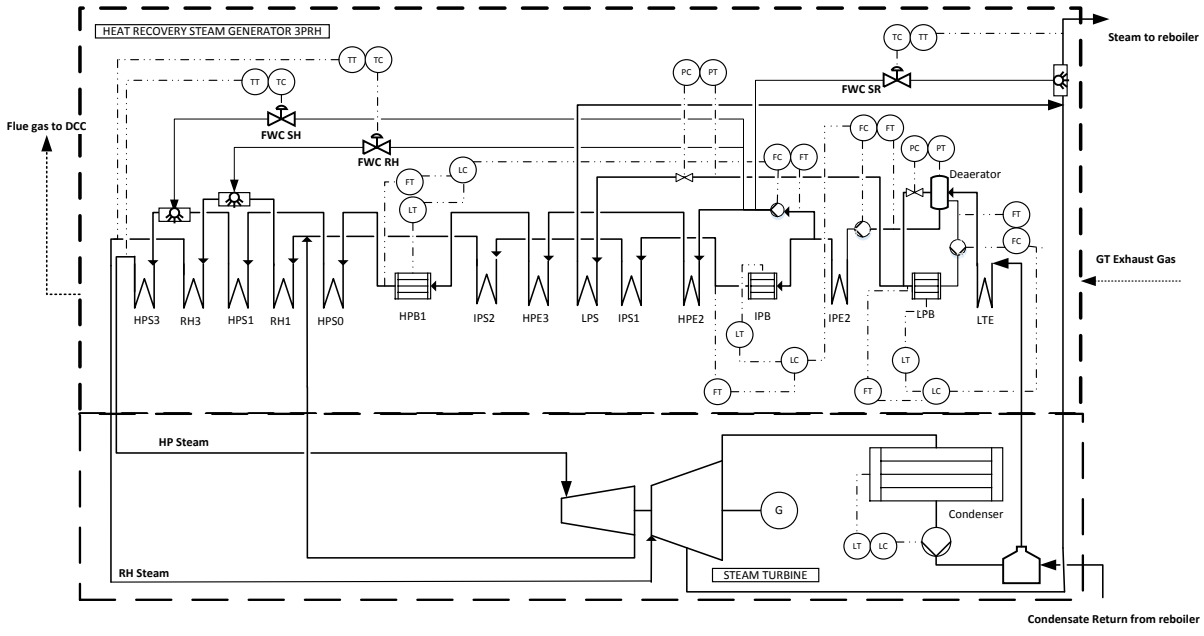

Figure 4. Power plant control layers. For controllers, the first letter stands for temperature (T), pressure (P), level (L) or flow rate (F), while the second letter stands for controller (C) or transmitter (T).

• Live-steam temperature control (FWC-SH, FWC-RH and FWC-SR): The temperature of the live steam (superheated, reheated and steam sent to reboiler) must be controlled to limit the temperature peaks that occur during off-design operation. High pressure feedwater is injected in between the superheaters and reheaters into the live steam to cool it down. In this work, proportional and integral (PI) controllers on control valves were implemented. The superheated steam sent to the reboiler must come at suitable temperatures required for the proper operation of the reboiler. Therefore, it was controlled by injecting high-pressure feedwater from the HRSG with a PI controller on a control valve.

• Drum level control: A three-element controller was applied for the three drums (LP, IP and HP) in the process. Drum level, feedwater and live-steam flows are measured. These signals were processed in a cascading manner [63] so that the controllers decide on the feedwater valves' opening.

• The pressure of the LP drum and that of the deaerator are controlled; refer to Figure 4.

• A level controller was applied to the condenser howtwell; refer to Figure 4.

5.2. Control layers of the post-combustion plant

Rules for consistent inventory control were followed [61] in order to design the regulatory control layer of the PCC system. An important decision is to select the location of the throughput manipulator for the amine/water solvent circulation, i.e., the mass flow rate of the recycled solvent circulating though absorber and stripper. For this configuration with two absorbers in parallel, there are two throughput manipulators (TPMs). Those two have been located at the inlet of the absorber; therefore, the TPMs are the solvent flow rates at the inlet of the absorbers $F_{s,a}$ and $F_{s,b}$. This defines the direction of the level controllers for absorber sumps and stripper sump. For this process configuration, the main drifting variables that need to be controlled to ensure stable operation of the PCC plant are:

- Rich solvent temperatures at the inlet of the absorbers.
- Absorber sumps and stripper sump levels.
- Stripper pressure.
- Condenser temperature.
- Reboiler steam/water side level.
- Make-up water.

The "pairings" or inputs utilized to control the above-mentioned drifting variables are shown in Figure 5. During pilot plant operation, MEA concentration is manually monitored onsite by periodic lab samples. MEA concentration is adjusted to (30 wt%) by the addition or extraction of water [64]. For practical implementation in the dynamic process model, the water injected/rejected from the PCC plant is the amount required to have a water mass balance of the overall PCC plant; water is added/rejected in the surge tank based on the measured water flow rate inlet to the absorbers, outlet to the absorbers and outlet to stack. MEA make-up was not introduced because the process model assumes that MEA is non-volatile and does not leave the plant through the absorber.

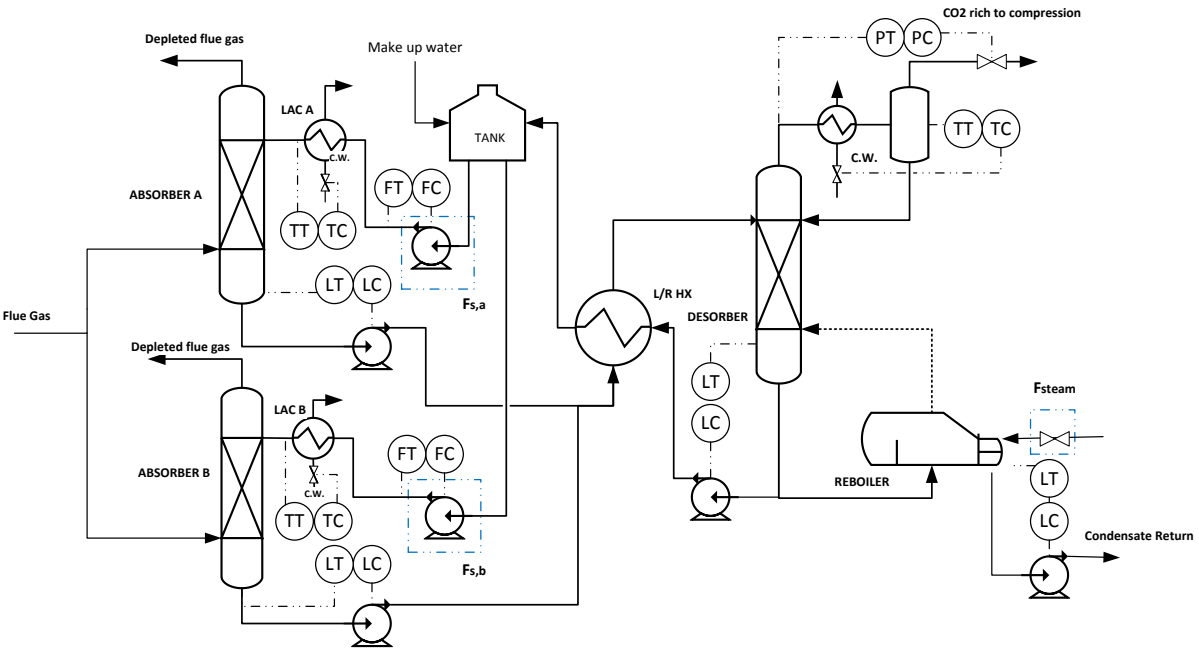

Figure 5. Control layer of the post-combustion capture system. $F_{s,a}$, $F_{s,b}$ and F_{steam} are the main degrees of freedom of the plant. For controllers, the first letter stands for temperature (T), pressure (P), level (L) or flow rate (F), while the second letter stands for controller (C) or transmitter (T).

The supervisory control layer of the PCC plant for this process configuration has three degrees of freedom, consisting of lean solvent flow rates to the absorber $F_{s,a}$ and $F_{s,b}$ and steam mass flow rate to the reboiler F_{steam}. These degrees of freedom will be used to control different process variables, depending on the operational strategy and objectives of the plant. Based on a literature study, five decentralized control structures were studied for load-change operation of the full power plant with PCC; refer to Table 6. Choosing appropriate tuning rules is of importance. Controller tuning was carried out based on simplified internal model control (SIMC) tuning rules, which are analytically derived and are well-suited for processes with large dead times and long stabilization times [65].

Panahi and Skogestad [22, 25] carried out a plant-wide control procedure for the post-combustion capture process with flue gas from a coal-fired power plant source, based on self-optimizing control theory [60]. Their study concluded that the two main self-optimizing control variables (CVs) are the CO_2 capture rate *Cap* at the outlet of the absorber and the temperature of a tray within the stripper (T_{str}). They evaluated four decentralized control structures based on different pairings of the above mentioned manipulable variables (MVs) and CVs and different regions of operation of the plant. They also evaluated a model predictive control scheme (MPC), concluding that MPC might not be required for base-load operation. Nittaya et al. [23] evaluated three different control structures under disturbances from coal-fired power plants with absorber-desorber PCC system; they studied different control structures based on a static relative gain array [66] analysis and heuristic approaches. The control structures were evaluated under different scenarios, including CO_2 capture rate set-point change and changes in flue gas flow rate. Their study concludes that decentralized control structures A and B (see Table 6) showed the best performance in respect of disturbances and set-point tracking, considering different operational objectives. Control structures *A* and *B* have CO_2 capture rate at top of absorber columns as CVs, see Table 6, and were selected for further study with the integrated dynamic process model of the power plant. The results are presented in Scenario 2 Case 1, in Section 6.2.1.

In addition, control structures in which the CO_2 capture rate is not a constraint or operational objective were studied. Since changes in solvent circulation rate can result in large dead times and total stabilization times of the main process variables of the plant [21], control structure *C* with constant solvent circulation rates was studied. In addition, ratio control on solvent circulation rate to keep

constant liquid to gas (L/G) ratio in the absorber at part-load operation was considered, with T_{reb} controlled by F_{steam} (structure *D*) and ratio control on F_{steam} (structure *E*), as proposed in [67]. The results are presented in Scenario 2 Case 2, in Section 6.2.2.

Table 6. Control structures for the PCC plant studied in this work.

Structure	**A**			**B**			**C**			**D**			**E**		
MV	$F_{s,a}$	$F_{s,b}$	F_{steam}	$F_{s,a}$	$F_{s,b}$	F_{steam}	$F_{s,a}$	$F_{s,b}$	F_{steam}	$F_{s,a}$	$F_{s,b}$	F_{steam}	$F_{s,a}$	$F_{s,b}$	F_{steam}
CV	Cap_a	Cap_b	T_{reb}	T_{reb}	T_{reb}	Cap_a	$F_{s,a}$	$F_{s,b}$	T_{reb}	L/G_a	L/G_b	T_{reb}	L/G_a	L/G_b	$F_{steam}/F_{s,a}$

6. Results and discussion

6.1. Scenario 1: Performance of the NGCC-PCC during load change

The transient performance of the integrated power plant during load change driven by GT load reduction was studied for different ramp rates. These simulations represent the operation of the plant when following a scheduled power output change established in a day-ahead power market [59]. The plant operator will change the power plant load set-point, and the transience will be driven by GT load change. In this study we consider load change from 100% GT load to 85% GT load. The ramp rates are chosen to represent a slow change of 2%/min GT load; a typical load change in NGCC power plant operation is 5%/min GT load reduction [14, 17], and a more aggressive load change of 10%/min GT load is utilized in modern fast cycling combined cycle power plants [14]. For this scenario, the PCC unit is operated with control structure A, according to Table 6. The transient gross power output of the gas turbine, steam turbine and combined cycle plant is presented in Figure 6. Figure 7 shows the HP and IP pressures at the steam turbine intake during load change. Table 7 shows 100% rise times and 99.9% settling times for GT power output and steam turbine (ST) power output for different GT ramp rates. Rise time is a measure on how fast the response of the process variable to load change is in the short timescales of 10^0-10^1 min, characteristic of the transient operation of NGCC power plant during load change [47]. Here, rise time means the time required for the response changing from 0% to 100% of its final value. In addition, the settling time is a good indicator of the long total stabilization time of the process variables, which propagate to the longer timescales, 10^1-10^2 min, normally observed in PCC process load change transient operation [21]. Settling times refer to the time required for the response curve to reach and stay within a range of 0.1% of the final value.

Table 7. Rise times and settling times for main power plant and PCC unit process variables.

	2%/min		**5%/min**		**10%/min**	
Variable	**Rise time 100 % [min]**	**Settling time 99.9 % [min]**	**Rise time 100 % [min]**	**Settling time 99.9 % [min]**	**Rise time 100 % [min]**	**Settling time 99.9 % [min]**
GT Power	7.5	7.4	3	2.9	1.5	1.4
ST Power	9.9	160	6.5	160	3.7	160
HP Pressure	13.2	13.2	8.9	8.9	7.6	7.6
IP Pressure	11.0	21.2	7.7	20	6.9	18
Steam Extraction to reboiler	73.3	301.15	73.3	301.5	70	301.5
Product CO_2 flow	78.33	292.9	9.5	292.9	8.6	292.9

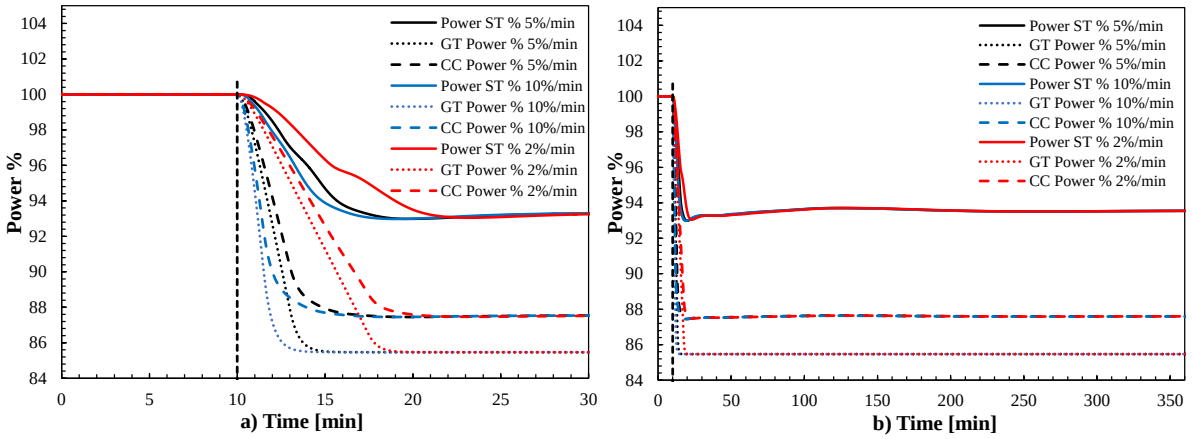

Figure 6. Scenario 1: Percentage of power output with respect to nominal values for steam turbine (ST), gas turbine (GT) and the total combined cycle (CC). Three scenarios for load change driven by GT load reduction (100% to 85%) at three different ramp rates are: conservative (2%/min), typical for modern NGCCs (5%/min) and modern NGCCs with fast cycling concepts (10%/min). The vertical dotted line shows when the load change begins. Note that the only change in the figure a to b is on the timescale and range (axis-of-abscissas).

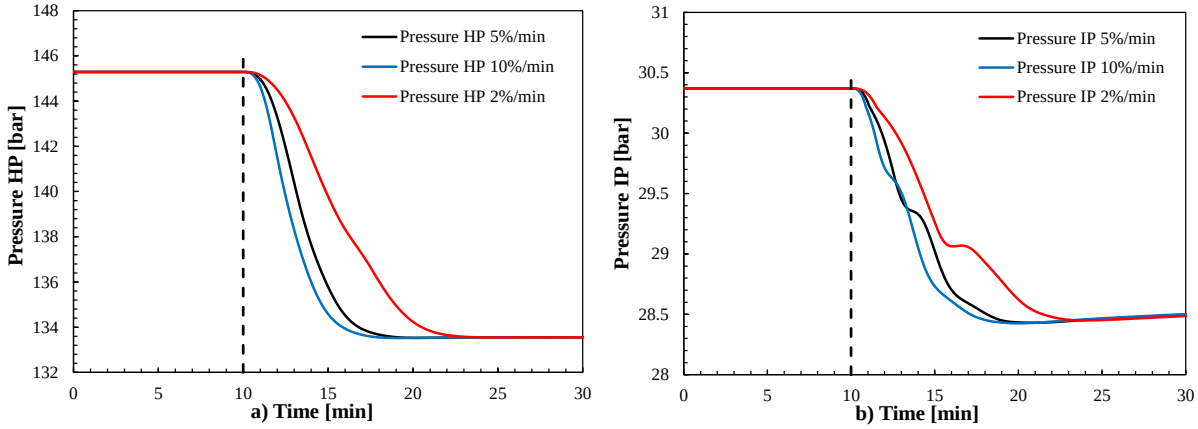

Figure 7. Scenario 1: HP and IP pressures at steam turbine intakes during load change driven by GT load reduction, for three different ramp rates (2%/min, 5%/min and 10%/min).

Figure 6a shows that, after a GT load reduction, the ST power output is reduced with a longer rise time, in the range of 4 to 9 minutes instead of the 2-8 min of the GT, see Table 7. This shows the effect of the mass and energy storage of the HRSG and other components of the power plant on the transient response of the steam cycle. The faster the GT load change ramp rate, the faster the change in ST and total CC power output of the power plant. In addition, with faster ramp rate, the difference between the GT and ST rise times will be larger. Figure 6b shows slow oscillations with small amplitude (<1%) in the ST transient response. Slow here means in the order of 160 min, clearly within the timescales of chemical plant operation. This is explained by the fact that the steam extraction is regulated by a throttle valve that is used as a MV to regulate a CV of the PCC unit, in this case T_{reb}. This means that there is a dynamic interaction between the power plant and the PCC unit in the longer timescales (10^1 to 10^2 min). The time-dependent trajectory of the steam mass flow rate extraction for different GT load ramp rates is presented in Figures 8e and 8f. It should be mentioned here that the contribution made by the GT to total CC power output is 74.8 % at 100% GT load and 71.9% at 85% GT load. This proportion is larger than for combined cycles without post-combustion capture (around 2/3 GT power at high GT loads), since the steam extraction from the IP/LP turbine represents around 50% of the total steam mass flow rate through the LP turbine. This means that the highest contribution to total power output of the power plant is provided by the GT. Hence, the ST's slower stabilization time loses importance when compared with the total power output of the power plant.

The sliding pressure operation mode of the HRSG is demonstrated in Figure 7, where it is shown that the ST intake pressures vary over time for different GT load change ramp rates. The transient response of ST intake pressures varies for different GT load ramp rates, there being faster rise time and settling time for faster GT ramp rates. This transient response can be explained by the HRSG thermal inertia, added mainly by mass and energy storage phenomena in large lumped metal mass walls and fluids within the drum boilers and recuperators. In addition, the rise time and settling time for HP and IP pressures remain within the timescale for power plant operation; see Table 7. Consequently, for these main process variables in the power plant, it can be said that there is no interaction between the power plant and the PCC unit.

Figure 8 shows the transient performance of the main process variables of the PCC unit during the GT driven load change. The CO_2 capture rate measured at the top of the absorbers, as in Equation (8), is shown in Figure 8a (short timescale) and Figure 8b (long timescale). It can be seen that the power plant load change has a strong effect on the PCC unit's load change, mainly through the fast reduction of GT exhaust mass flow rate that propagates towards the HRSG, fan, DCCs and absorber columns. Hence, the GT load change imposes the load change of the PCC unit within the timescales of power plant operation (10^0-10^1 min). The CO_2 capture rate depend on the ramp rates. The faster the ramp rate, the larger the amplitude of oscillations in the CO_2 capture rate in the short timescales (Figure 8a), while a similar amplitude of oscillations is found in the longer timescales (Figure 8b). A similar trend is found in the uncontrolled CO_2 rich product mass flow rate and in the steam extraction mass flow rate; refer to Figures 8c-f. The reboiler solvent temperature, shown in Figures 8g-h, is properly controlled within reasonable limits, so no excessive solvent thermal degradation can be expected under transient load change.

$$Cap = \frac{\dot{F}_{abs,in} \cdot X_{in,CO_2} - \dot{F}_{abs,out} \cdot X_{out,CO_2}}{\dot{F}_{abs,in} \cdot X_{in,CO_2}} \quad (8)$$

6.2. Scenario 2: Performance of different PCC plant control structures under power plant load change

6.2.1. Case 1: CO_2 capture rate to 90% as a control objective

In this case the CVs, Cap_a, Cap_b and T_{reb}, are to be controlled by means of the remaining degrees of freedom or MVs, those being $F_{s,a}$, $F_{s,b}$ and F_{steam}. As shown in Table 6, control structure A pairs solvent circulation flows with capture rates at the top of the absorber and F_{steam} with T_{reb}, whereas control structure B pairs solvent circulation flow rates with T_{reb} and F_{steam} with capture rate Cap. The transient performance of the power plant integrated with PCC for these two control structures is tested for a typical GT load change with a ramp rate of 5%/min down and up, of the range of 100% GT load to 75% GT load; refer to Figures 9 - 11. Rise times and settling times for the transient events are presented in Table 8.

Steam turbine power output is shown in Figure 9a and 9b. It can be observed that the five different decentralized control structures show similar responses in terms of steam turbine power output transient performance in the short timescales (10^0-10^1), with similar rise times. This means that, in the shorter timescale, the response of the power plant is similar from a dynamic perspective for the different control structures. However, steam turbine power output settling times are larger for structures A and B, where Cap_a and Cap_b are controlled to the set value of 90%. In addition, a slow response in terms of CO_2 product mass flow rate is observed for both control structures A and B.

Total stabilization times for this process variable range from around 3 – 4 hours for structure A and around 7 – 10 hours for structure B. When utilizing control structure A, the CO_2 product mass flow rate rise time remains within the shorter timescales of thermal power plant operation, being faster than for structure B (Figures 9c-d).

Figure 10 shows the input usage required to operate the PCC unit during transient load change, i.e. solvent circulation mass flow rates for each of the absorbers and steam circulation flow rate. The stabilization of input usage process variables or MVs is clearly slower when CO_2 capture is an objective for plant operation, structure B being slower; see also Table 8. This might explain the slower response of steam turbine power output due to slower steam extraction mass flow rate stabilization time. In addition, Figure 11 shows the controlled variables, Cap_a, Cap_b and T_{reb}, for the different control structures. It can be seen how structure A shows superior performance, when comparing the CO_2 capture rate response to a disturbance driven by GT load change, and it can be said that structure A would lead to more efficient operation during transient load change. The faster response of the main plant process variables to GT load change when implementing control structure A can be explained by that structure A has faster closed feedback control loops. This means that the paired MVs and CVs are physically closer, which results in tight control when compared with control structure B. It can be observed in Figure 10 that the manipulated variables, $F_{s,a}$, $F_{s,b}$ *and* F_{steam}, reach faster stabilization for control structure A than for control structure B; also refer to rise times and settling times for steam extraction mass flow rate presented in Table 8.

6.2.2. Case 2: CO_2 capture rate to 90% is not a control objective

In this case the CVs, Cap_a and Cap_b, at the top of the absorbers are not a control objective, leading the remaining degrees of freedom or MVs for control of another process variable.

Studies consisting of the plant's open-loop response to step changes in solvent circulation rate have shown that the main process variables of the PCC plant have long stabilization times, mainly due to the large residence times in components that contain large inventories of solvent and long dead times within piping and process hold-ups [21]. In addition, the dynamic interaction between the absorber and reboiler operation might lead to large total stabilization times. Hence, slow stabilization of the plant are expected when the liquid solvent flow network is disturbed. This can explain why the utilization of the solvent circulation rate, as a MV to regulate a control variable in feedforward (ratio) or closed-loop feedback control, might lead to large total stabilization times of the PCC unit's main process variables. Therefore, it can be reasonable to believe that leaving the MVs' solvent circulation rates at the top of the absorber in flow control mode might lead to a faster plant (keeping circulation flow rate constant as in Figure 9 c) and d) with control structure C). However, even if the plant stabilizes relatively quickly when keeping the solvent flow network unaltered, the plant is operated in a less efficient manner under off-design loads. This is shown in Figures 9-11, where it can be seen that, for the steady-state off-design conditions of 75% GT load, lower steam turbine power output is obtained, in addition to larger steam extraction mass flow rate (and reboiler duty) and therefore large CO_2 capture rate of around 97%. It must be said that, for structure C, it is not possible to keep the reboiler temperature at set-point, since the steam valve stem saturates and no further steam can be sent to the reboiler at the part-load operation point of 75% GT load. At part load operating conditions, less steam was available for the extraction from the ST. In addition, a large solvent circulation flow rate (large L/G ratio) was obtained when solvent circulation $F_{s,a}$ and $F_{s,b}$ were kept constant. That lead to relatively larger steam extraction and reboiler duty required for operation of the process, as observed in control structure C, refer to Figure 10. In addition, control structure E showed faster stabilization response to the disturbance than control structures A and B, see Table 8. However, control structure E lead to relatively larger L/G ratio in the absorber columns when compared to A, B and D, and therefore a sub-optimal operation of the process with a larger steam extraction required and resulting capture rate.

Structure D utilizes solvent flow rates on L/G ratio control mode (feedforward). The mass based L/G ratio in the absorber columns is kept constant at off-design loads by using the lean solvent flow rates' MVs. This results in the fast change and stabilization of solvent circulation rate, as shown in Figure 10, that follows the exhaust gas mass flow rate reduction of the GT. In addition, this also leads to faster stabilization of steam extraction F_{steam} than for control structures A and B; refer to rise times and settling

707 times in Table 8. By looking at the steady-state off-design performance of the PCC unit when operated
708 with GT load of 75%, it can be seen that the CO_2 capture rate is kept almost constant when the L/G ratio
709 is kept constant. In steady-state terms, the plant's main process variables have a similar steady-state
710 value but significantly faster stabilization of reboiler solvent temperature, leading to faster stabilization
711 of CO_2 product flow rate and steam extraction flow rate; however, the CO_2 capture rate is slower than
712 when compared with CO_2 capture controlled as in structure A. Therefore, the L/G ratio control, as in
713 structure D, can be considered as a good option if relatively fast stabilization times in CO_2 product flow
714 rate and steam turbine power output are required simultaneously, while keeping the CO_2 capture rate
715 close to 90% at part-load operation.

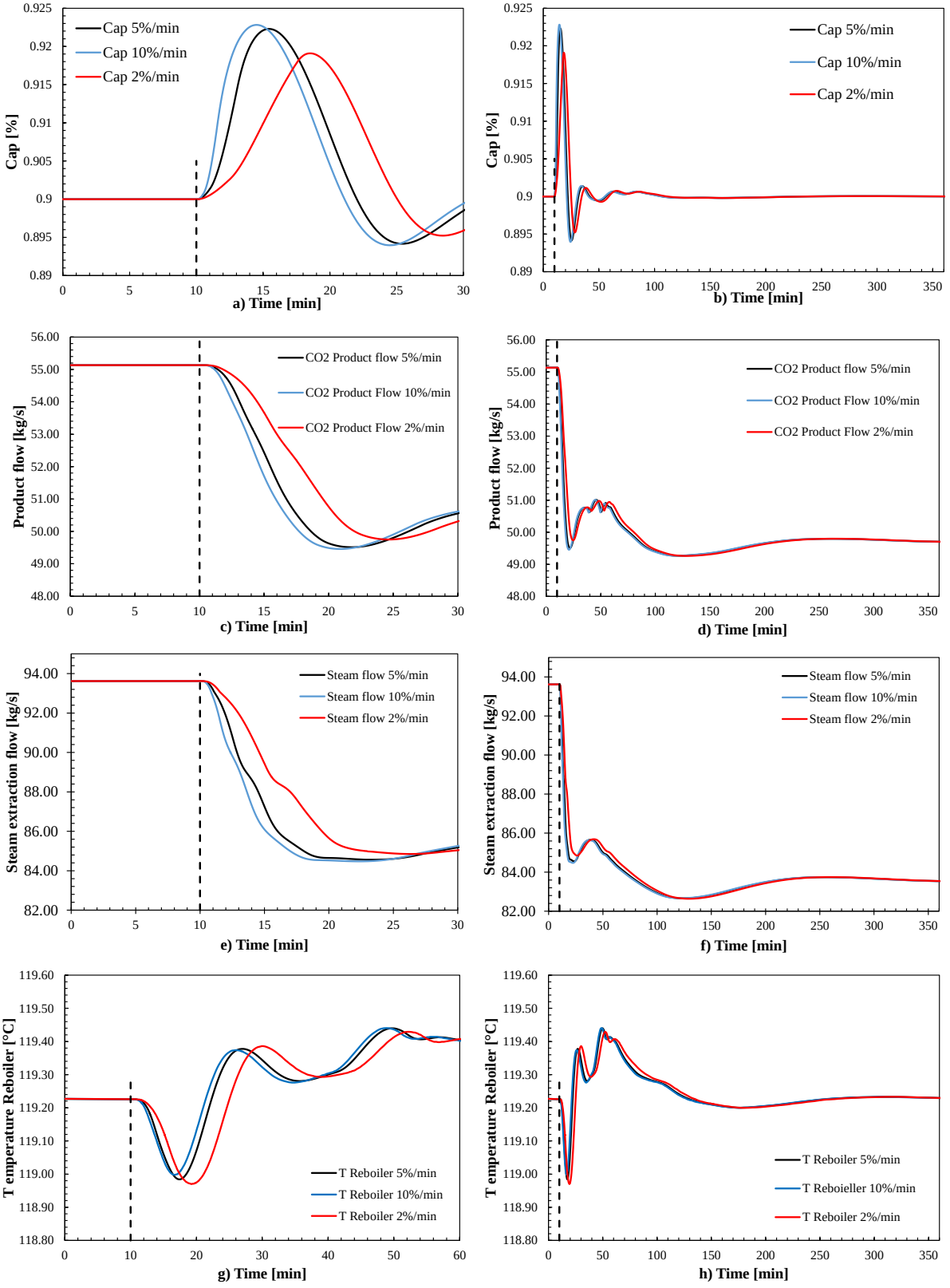

Figure 8. Scenario 1: Main process variables of the post-combustion capture system during load change driven by GT load reduction for different GT ramp rates. For these simulations, control structure A was implemented, refer to Table 6. Left figures include timescales on thermal power plant operation, while right figures show timescales for interest on post-combustion capture system operation Note the differences on the timescale and range (axis-of-abscissas).

Control structure E uses feedforward ratio control for both steam mass flow rate and solvent circulation mass flow rate, by keeping constant the mass based L/G ratio in the absorber and the ratio of steam extraction mass flow rate to solvent circulation mass flow rate at the inlet of the absorbers; see Table 6. Figure 10 shows that the MVs quickly follow the change in exhaust gas mass flow rate imposed by GT load change. CO_2 product mass flow rate and steam turbine power output have similar settling times and transient trajectories for structures D and E. However, structure D leads to a more efficient steady-state part-load operation, since structure E results in higher steam extraction flow rate – and hence more CO_2 being stripped from the solvent – and a larger CO_2 product flow rate. It seems that control structure D results in better performance than structure E under transient load change.

It should be mentioned that there is a significant difference between the trajectories, rise times and settling times of most process variables for a given control structure when ramping down (100% GT load to 75% GT load) and when ramping up (75% GT load to 100% GT load). This highlights the fact that the dynamic process system is highly non-linear.

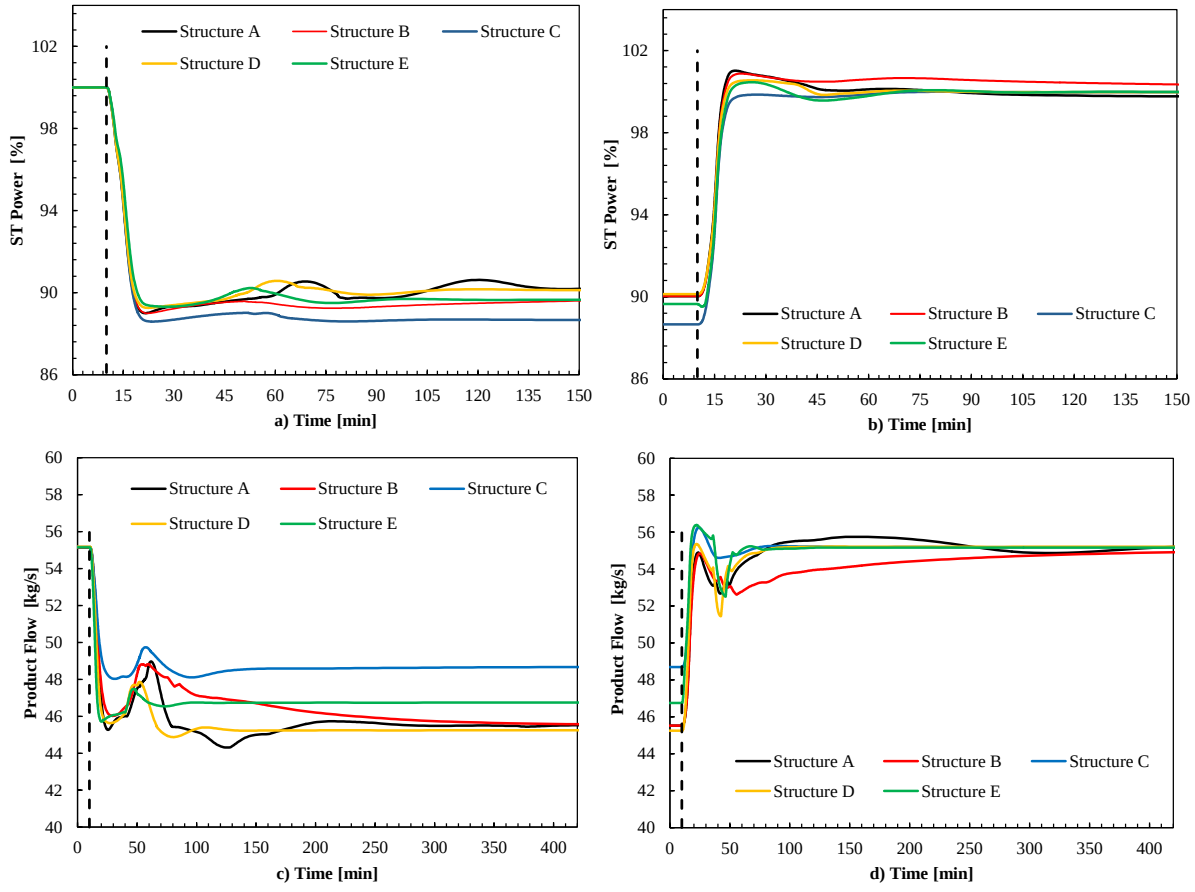

Figure 9. Scenario 2: Transient response of different control structures to GT load change with 5%/min ramp rate reduction and increase. Steam turbine power output [%] a) and b), and CO_2 product flow [kg/s] c) and d). Note the difference in timescale in the axis-of-abscissas.

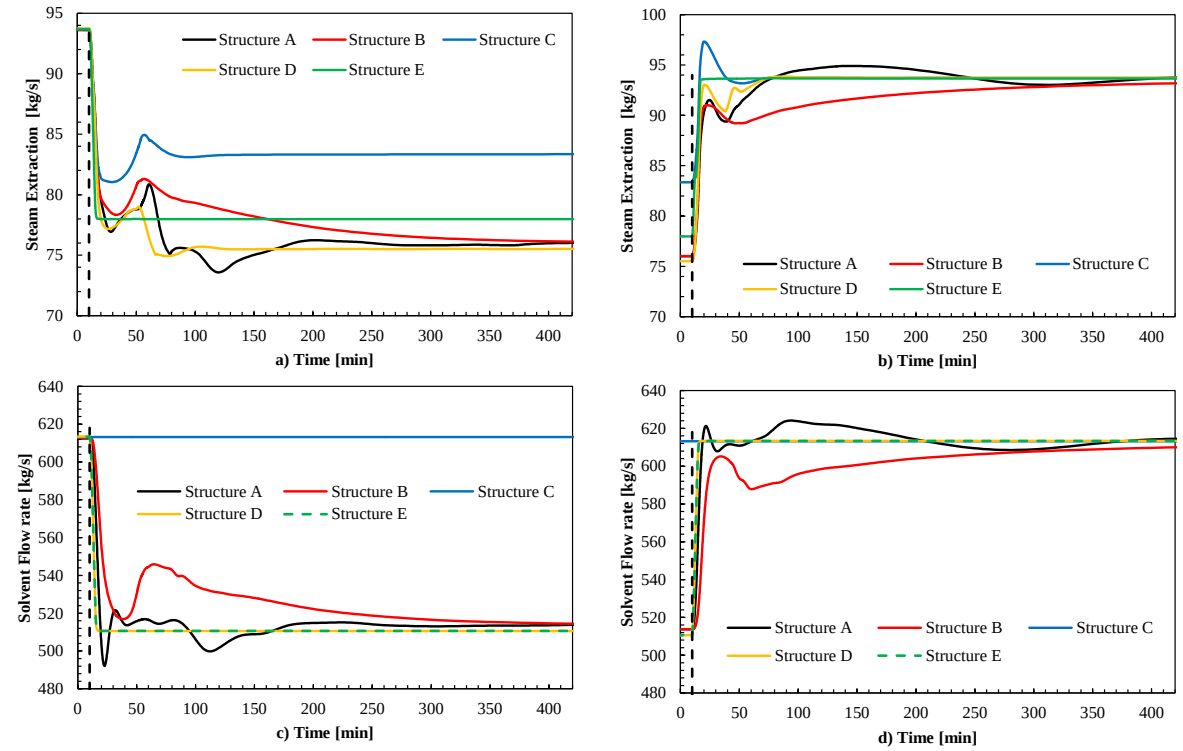

739

740 *Figure 10. Scenario 2: Steam turbine extraction flow rate [kg/s] a) and b), and solvent flow rate [kg/s] c) and d).*
741 *Transient response of different control structures to a 5%/min ramp rate GT load reduction (a) and c)) and*
742 *increase (b) and d)).*

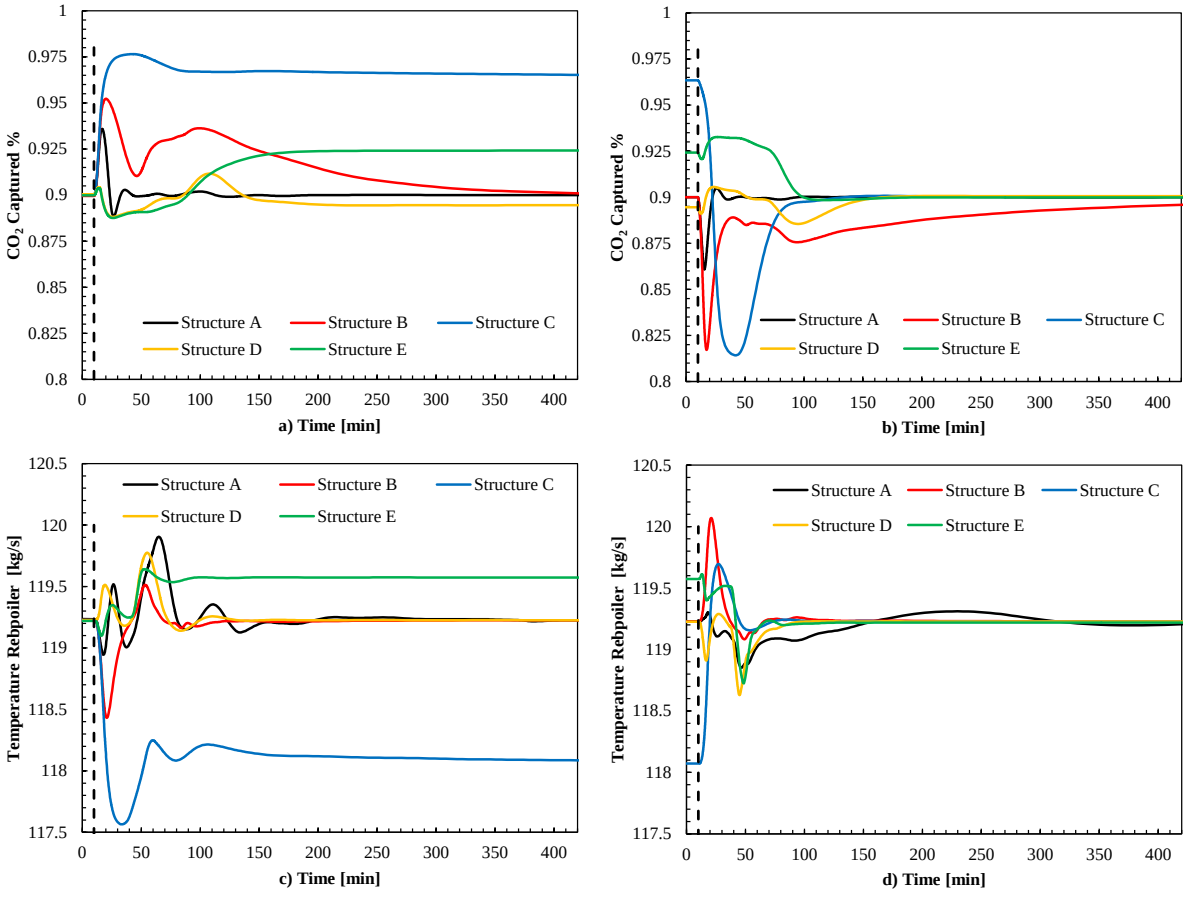

743

744 *Figure 11. Scenario 2: CO_2 capture rate [%] a) and b),* and solvent temperature in reboiler *[°C] c) and d).*
745 *Transient response of different control structures to a 5%/min ramp rate GT load reduction (a) and c)) and*
746 *increase (b) and d)).*

747 *Table 8. Rise times and settling times for different process variables with different control structures of the*
748 *integrated power plant with PCC for GT load change at 5%/min ramp rate. GT load decrease from 100% to 75%*
749 *and GT load increase from 75% to 100%. Times in min.*

Variable		ST Power	CO_2 capture rate	Steam Extraction to reboiler	Product CO_2 flow
Structure A					
Rise time 100% [min]	Down	7.9		63.4	12.9
	Up	7.7		67.26	72.1
Settling time 99.9% [min]	Down	164.7		484.7	175.6
	Up	321.5		530.7	242.9
Structure B					
Rise time 100% [min]	Down	8		148.3	412.5
	Up	8.1		658	658.1
Settling time 99.9% [min]	Down	278		435.9	412.5
	Up	356		658	658.1
Structure C					
Rise time 100% [min]	Down	11.3	9.3	6.8	12.1
	Up	19	12.3	6.3	9.3
Settling time 99.9% [min]	Down	54.7	381.8	11.5	317.2
	Up	50.4	114.3	81.3	61.4
Structure D					
Rise time 100% [min]	Down	8.1	8.4	53.9	120.3
	Up	8.6	7.2	65.3	10.4
Settling time 99.9% [min]	Down	61.4	45	108.4	251.7
	Up	40.1	153.3	65.3	79.2
Structure E					
Rise time 100% [min]	Down	10.1	274.1	9.4	6.7
	Up	9.23	89.55	11.51	27.4
Settling time 99.9% [min]	Down	55.3	274.1	9.4	48
	Up	53.4	89.55	9.4	92.05

750

751 ## 7. Conclusions

752 Understanding the dynamic interaction between the NGCC power plant and the PCC unit remains a key
753 aspect when developing the NGCC with PCC technology. This work simulates real-like operation of a
754 3PRH natural gas combined cycle power plant with post combustion capture during load change
755 transient event with closed-loop controllers. In addition, this work includes detailed dynamic process
756 models of the power plant to the same level of detail as in the chemical absorption and desorption plant.

757 The performance of the integrated NGCC power plant with PCC for different GT load change ramp
758 rates was demonstrated and assessed via dynamic process model simulations. When the steam extraction
759 mass flow rate is regulated by a throttle valve, which is used as a MV to control a CV of the PCC unit,
760 dynamic interaction is found between the power plant and the PCC unit in the longer timescales, 10^1 to
761 10^2 min. Slow oscillations with relatively small amplitude are found in the power production from the
762 steam turbine. These oscillations in the long timescales are within (<1%) of total ST power output. In
763 addition, the GT load change imposes the load change of the PCC unit within the timescales of power

plant transient operation of 10^0-10^1 min, due to the fast reduction of exhaust mass flow rate from the GT during load change. Faster GT ramp rates cause faster rise times in the power plant process variables. For different GT ramp rates, different trajectories of the main process variables of the PCC unit are found within the timescales of power plant transient operation. Nevertheless, within the longer timescales of 10^1- 10^2, the transient performance of the PCC unit is similar for different GT ramp rates. Based on these simulations, it can be concluded that the addition of the PCC unit to the NGCC plant should not impose any constraint on, or problem for, stable power plant operation under scheduled load changes, nevertheless inefficient transient operation of the PCC unit can be expected in the long timescales.

The transient performance of five different decentralized PCC plant control structures under power plant load change was assessed. It is observed that the control structures display similar performance in terms of steam turbine power output in the short timescales (10^0-10^1), with similar rise times, while, in the longer timescales, the steam turbine power output differs for different control structures. This means that, within shorter timescales, the response of the power plant is similar from a dynamic perspective for the different control structures. When controlling the CO_2 capture rate, the power plant performs in a more efficient manner at steady-state off-design loads; however, the time-dependent response of the PCC plant is slower, leading to long stabilization times in the main process variables. The control structure where L/G ratio is kept constant and reboiler temperature is controlled by the steam throttle valve, has shown similar part-load off-design performance as that found in control structures with constant capture rate as CVs. In addition, this control structure results in relatively fast total stabilization time of the steam turbine power output and CO_2 product flow rate. It is recommended to apply control structure D, with L/G ratio control, if controlling CO_2 capture rate is not an operational constraint.

Acknowledgements

This work has been financially supported by the Department of Energy and Process Engineering at the NTNU – Norwegian University of Science and Technology. The authors also acknowledge the Chalmers Energy Initiative, the Swedish Energy Agency and Landsvirkjun Energy Research Fund for funding parts of this project.

Nomenclature, abbreviations and subscripts

AP	Absolute percentage error
Ar	Argon
Cap	Capture rate *[%]*
CCS	Carbon capture and storage
CH_4	Methane
CO_2	Carbon dioxide
CV	Control variable
CW	Cooling water
DA	Deaerator
DCC	Direct contact cooler
EGR	Exhaust gas recycle
F	Mass flow rate *[kg/s]*
F_a	Arrangement factor
FWC	Feedwater cooler
GHG	Greenhouse gas

GT	Gas turbine
h	Enthalpy *[J/kg]*
HP	High pressure
HPB	High pressure boiler
HPE2	High pressure economizer 2
HPE3	High pressure economizer 3
HPS0	High pressure superheater 0
HPS1	High pressure superheater 1
HPS3	High pressure superheater 3
HRSG	Heat recovery steam generator
H_2O	Water
IP	Intermediate pressure
IPB	Intermediate pressure boiler
IPE2	Intermediate pressure economizer
IPS1	Intermediate pressure superheater 1
IPS2	Intermediate pressure superheater 2
K_b	Bauman factor
K_t	Flow area coefficient
LAC	Lean amine cooler
L/G	Liquid to gas ratio *[kg/kg]*
LHV	Lower heating value
LP	Low pressure
LPB	Low pressure boiler
LPS	Low pressure superheater
LTE	Low temperature economizer
MAP	Mean absolute percentage error
MEA	Monoethanolamine
MPC	Model predictive control
MV	Manipulable variable
NGCC	Natural gas combined cycle
NO_x	Nitrogen oxides
N_2	Nitrogen
O_2	Oxygen
PCC	Post-combustion CO_2 capture
reb	Reboiler
RH1	Reheater 1
RH3	Reheater 3
RGA	Relative gain array
s	Solvent

SIMC	Simplified internal mode l control
ST	Steam turbine
SO_2	Sulfur oxides
T	Temperature *[K]*
TET	Turbine exhaust temperature
TIT	Turbine inlet temperature
TPM	Throughput manipulator
VIGVs	Variable inlet guide vanes
wt	Weight percent *[kg/kg]*
x	Vapor quality *[kg/kg]*
X	Mass fraction *[kg/kg]*
3PRH	Three-pressure reheat
Greek symbols	
η	Efficiency
ρ	Density $[kg/m^3]$
λ	Thermal conductivity *[W/m K]*

References

[1] IPCC, Climate Change 2013: The Physical Science Basis. Contribution of Working Group I to the Fifth Assessment Report of the Intergovernmental Panel on Climate Change, Cambridge University Press, Cambridge, United Kingdom and New York, NY, USA, 2013.
[2] IPCC, Climate Change 2014: Synthesis Report. Contribution of Working Groups I, II and III to the Fifth Assessment Report of the Intergovernmental Panel on Climate Change, in, IPCC, Geneva, Switzerland, 2014, pp. 151 pp.
[3] IEA, World Energy Outlook 2015, OECD Publishing.
[4] T. Dixon, H. Herzog, S. Twinning, N. Ceccarelli, M. van Leeuwen, T. Wolf, P. van Leeuwen, R. van der Vaart, W. Maas, A. Ramos, 12th International Conference on Greenhouse Gas Control Technologies, GHGT-12Flexibility of Low-CO2 Gas Power Plants: Integration of the CO2 Capture Unit with CCGT Operation, Energy Procedia, 63 (2014) 1703-1726.
[5] B.F. Möller, M. Genrup, M. Assadi, On the off-design of a natural gas-fired combined cycle with CO2 capture, Energy, 32 (2007) 353-359.
[6] IEAGHG, Operating Flexibility of Power Plants with CCS, in, IEAGHG, June 2012.
[7] G.T. World, 2016 Performance Specs, 32nd Edition, in: Gas Turbine World, Pequot Publishing Inc., Fairfield, USA, 2016, pp. 48.
[8] IEA, World Energy Investment 2016, in, 2016.
[9] F. Johnsson, M. Odenberger, L. Göransson, Challenges to Integrate CCS into Low Carbon Electricity Markets, Energy Procedia, 63 (2014) 7485-7493.
[10] IEA, CO2 Capture and storage: A key carbon abatement option, in: Energy Technology Analysis, International Energy Agency, 2008.
[11] T. Adams, N. Mac Dowell, Off-design point modelling of a 420 MW CCGT power plant integrated with an amine-based post-combustion CO2 capture and compression process, Applied Energy, 178 (2016) 681-702.
[12] IEA, Harnessing variable renewables: A guide to the balancing challenge, in, International Energy Agency, 2011.
[13] A.S. Brouwer, M. van den Broek, A. Seebregts, A. Faaij, Operational flexibility and economics of power plants in future low-carbon power systems, Applied Energy, 156 (2015) 107-128.
[14] M. Genrup, M. Thern, Ny gasturbinteknik 2012-2014: Gas Turbine Developments. Report 2012., in, ELFORSK, March 2013.
[15] IEAGHG, Evaluation of process control strategies for normal, flexible, and upset operation conditions of CO2 post combustion capture processes. 2016/07, in, IEAGHG, September 2016.
[16] M.E. Boot-Handford, J.C. Abanades, E.J. Anthony, M.J. Blunt, S. Brandani, N. Mac Dowell, J.R. Fernandez, M.-C. Ferrari, R. Gross, J.P. Hallett, R.S. Haszeldine, P. Heptonstall, A. Lyngfelt, Z. Makuch, E. Mangano, R.T.J. Porter, M. Pourkashanian, G.T. Rochelle, N. Shah, J.G. Yao, P.S. Fennell, Carbon capture and storage update, Energy & Environmental Science, 7 (2014) 130-189.
[17] K. Jordal, P.A.M. Ystad, R. Anantharaman, A. Chikukwa, O. Bolland, Design-point and part-load considerations for natural gas combined cycle plants with post combustion capture, International Journal of Greenhouse Gas Control, 11 (2012) 271-282.
[18] K. Jonshagen, N. Sipöcz, M. Genrup, A Novel Approach of Retrofitting a Combined Cycle With Post Combustion CO2 Capture, Journal of Engineering for Gas Turbines and Power, 133 (2010) 011703-011703.
[19] R. Faber, M. Köpcke, O. Biede, J.N. Knudsen, J. Andersen, Open-loop step responses for the MEA post-combustion capture process: Experimental results from the Esbjerg pilot plant, Energy Procedia, 4 (2011) 1427-1434.
[20] M. Bui, I. Gunawan, V. Verheyen, P. Feron, E. Meuleman, S. Adeloju, Dynamic modelling and optimisation of flexible operation in post-combustion CO2 capture plants—A review, Computers & Chemical Engineering, 61 (2014) 245-265.
[21] N.E. Flø, H.M. Kvamsdal, M. Hillestad, T. Mejdell, Dominating Dynamics of the Post-combustion CO2 Absorption Process, Computers & Chemical Engineering.
[22] M. Panahi, S. Skogestad, Economically efficient operation of CO2 capturing process part I: Self-optimizing procedure for selecting the best controlled variables, Chemical Engineering and Processing: Process Intensification, 50 (2011) 247-253.
[23] T. Nittaya, P.L. Douglas, E. Croiset, L.A. Ricardez-Sandoval, Dynamic modelling and control of MEA absorption processes for CO2 capture from power plants, Fuel, 116 (2014) 672-691.
[24] M.S. Walters, T.F. Edgar, G.T. Rochelle, Regulatory Control of Amine Scrubbing for CO2 Capture from Power Plants, Industrial & Engineering Chemistry Research, 55 (2016) 4646-4657.

[25] M. Panahi, S. Skogestad, Economically efficient operation of CO2 capturing process. Part II. Design of control layer, Chemical Engineering and Processing: Process Intensification, 52 (2012) 112-124.
[26] E. Mechleri, A. Lawal, A. Ramos, J. Davison, N.M. Dowell, Process control strategies for flexible operation of post-combustion CO2 capture plants, International Journal of Greenhouse Gas Control, 57 (2017) 14-25.
[27] Z. He, L.A. Ricardez-Sandoval, Dynamic modelling of a commercial-scale CO2 capture plant integrated with a natural gas combined cycle (NGCC) power plant, International Journal of Greenhouse Gas Control, 55 (2016) 23-35.
[28] Thermoflow, GT Pro 24.0, in, Thermoflow Inc., 2014.
[29] A.T. Inc., Aspen Plus V8.6. , in, 2014.
[30] R. Dutta, L.O. Nord, O. Bolland, Selection and design of post-combustion CO2 capture process for 600 MW natural gas fueled thermal power plant based on operability, Energy, 121 (2017) 643-656.
[31] Z. Amrollahi, I.S. Ertesvåg, O. Bolland, Optimized process configurations of post-combustion CO2 capture for natural-gas-fired power plant—Exergy analysis, International Journal of Greenhouse Gas Control, 5 (2011) 1393-1405.
[32] N.E. Flø, Post-combustion absorption-based CO2 capture: modeling, validation and analysis of process dynamics, in: Chemical Engineering Department, Norwegian University of Science and Technology, Trondheim, 2015.
[33] H. Jilvero, A. Mathisen, N.-H. Eldrup, F. Normann, F. Johnsson, G.I. Müller, M.C. Melaaen, Techno-economic Analysis of Carbon Capture at an Aluminum Production Plant – Comparison of Post-combustion Capture Using MEA and Ammonia, Energy Procedia, 63 (2014) 6590-6601.
[34] M. Lucquiaud, H. Chalmers, J. Gibbins, Capture-ready supercritical coal-fired power plants and flexible post-combustion CO2 capture, Energy Procedia, 1 (2009) 1411-1418.
[35] M. Thern, K. Jordal, M. Genrup, Temporary CO2 Capture Shut Down: Implications on Low Pressure Steam Turbine Design and Efficiency, Energy Procedia, 51 (2014) 14-23.
[36] Z.A. Biyouki, Thermodynamic analysis of CO2 capture processes for power plants, in: Energy and Process Engineering, Norwegian University of Science and TEchnology, 2014.
[37] S. Linnenberg, U. Liebenthal, J. Oexmann, A. Kather, Derivation of power loss factors to evaluate the impact of postcombustion CO2 capture processes on steam power plant performance, Energy Procedia, 4 (2011) 1385-1394.
[38] F. Rezazadeh, W.F. Gale, K.J. Hughes, M. Pourkashanian, Performance viability of a natural gas fired combined cycle power plant integrated with post-combustion CO2 capture at part-load and temporary non-capture operations, International Journal of Greenhouse Gas Control, 39 (2015) 397-406.
[39] Modelica Association, https://www.modelica.org/, in.
[40] Modelon, ThermalPower Library, in, 2015.
[41] Dassault Systems, Dymola, http://www.3ds.com/products-services/catia/products/dymola, in.
[42] P.J. Dechamps, Modelling the Transient Behaviour of Heat Recovery Steam Generators, Proceedings of the Institution of Mechanical Engineers, Part A: Journal of Power and Energy, 209 (1995) 265-273.
[43] P.J. Dechamps, Modeling the transient behaviour of combined cycle plants, in: ASME paper 94-GT-238, 1994.
[44] W.I. Rowen, Simplified Mathematical Representations of Heavy-Duty Gas Turbines, Journal of Engineering for Power, 105 (1983) 865-869.
[45] S. Can Gülen, K. Kim, Gas Turbine Combined Cycle Dynamic Simulation: A Physics Based Simple Approach, Journal of Engineering for Gas Turbines and Power, 136 (2013) 011601-011601.
[46] W. Wagner, J.R. Cooper, A. Dittmann, J. Kijima, H.J. Kretzschmar, A. Kruse, R. Mareš, K. Oguchi, H. Sato, I. Stöcker, O. Šifner, Y. Takaishi, I. Tanishita, J. Trübenbach, T. Willkommen, The IAPWS Industrial Formulation 1997 for the Thermodynamic Properties of Water and Steam, Journal of Engineering for Gas Turbines and Power, 122 (2000) 150-184.
[47] A. Benato, A. Stoppato, A. Mirandola, Dynamic behaviour analysis of a three pressure level heat recovery steam generator during transient operation, Energy, 90, Part 2 (2015) 1595-1605.
[48] G.V.-G.V.u. Chemieingenieur-wesen, VDI-Wärmeatlas (VDI-Buch) (German Edition), 9th Edition ed., 1997.
[49] K.J. Åström, R.D. Bell, Drum-boiler dynamics, Automatica, 36 (2000) 363-378.
[50] J. Eborn, On Model Libraries for Thermo-hydraulic Applications, in: Deparment of Automatic Control, Lund Institute of Technology (LTH), Lund, 2001.
[51] A.L. Francesco Casella, Modelica open library for power plant simulation: design and experimental validation, in: P. Fritzon (Ed.) 3rd International Modelica Conference, Modelica Association, Linköping (Sweden), 2003, pp. 41-50.
[52] O. Bolland, Compendium - Thermal Power Generation, 2014.
[53] R. Kehlhofer, B. Rukes, F. Hannemann, F. Stirnimann, Combined-Cycle Gas and Steam Turbine Power Plants (3rd Edition), in, PennWell, 2009.
[54] Modelon, Post-combustion capture with amine solutions. http://www.modelon.com/industries/energy-process/carbon-capture-and-sequestration/, in.
[55] S.Ó. Garðarsdóttir, F. Normann, K. Andersson, K. Prölß, S. Emilsdóttir, F. Johnsson, Post-combustion CO2 capture applied to a state-of-the-art coal-fired power plant—The influence of dynamic process conditions, International Journal of Greenhouse Gas Control, 33 (2015) 51-62.
[56] K. Prölß, H. Tummescheit, S. Velut, J. Åkesson, Dynamic model of a post-combustion absorption unit for use in a non-linear model predictive control scheme, Energy Procedia, 4 (2011) 2620-2627.
[57] R.M. Montañés, N.E. Flø, R. Dutta, L.O. Nord, O. Bolland, Dynamic process model development and validation with transient plant data collected from an MEA test campaign at CO2 Technology Center Mongstad, Energy Procedia, (2017).
[58] CO2 Technology Center Mongstad, in.
[59] R.M. Montañés, M. Korpås, L.O. Nord, S. Jaehnert, Identifying Operational Requirements for Flexible CCS Power Plant in Future Energy Systems, Energy Procedia, 86 (2016) 22-31.
[60] S. Skogestad, I. Postlethwaite, Multivariable Feedback Control: Analysis and Design, John Wiley \& Sons, 2005.
[61] E.M.B. Aske, S. Skogestad, Consistent Inventory Control, Industrial & Engineering Chemistry Research, 48 (2009) 10892-10902.
[62] K. Jonshagen, Modern Thermal Power Plants. Aspects of modeling and evaluation, in: Division of Thermal Power Engineering. Department of Energy Science, Lund University, Lund, 2011.
[63] S. Basu, A.K. Debnath, Chapter VIII - Boiler Control System, in: Power Plant Instrumentation and Control Handbook, Academic Press, Boston, 2015, pp. 585-694.
[64] M. Bui, I. Gunawan, V. Verheyen, P. Feron, E. Meuleman, Flexible operation of CSIRO's post-combustion CO2 capture pilot plant at the AGL Loy Yang power station, International Journal of Greenhouse Gas Control.
[65] S. Skogestad, C. Grimholt, The SIMC Method for Smooth PID Controller Tuning, in: R. Vilanova, A. Visioli (Eds.) PID Control in the Third Millennium: Lessons Learned and New Approaches, Springer London, London, 2012, pp. 147-175.

[66] A.S. Chinen, J.C. Morgan, B.P. Omell, D. Bhattacharyya, D.C. Miller, Dynamic Data Reconciliation and Model Validation of a MEA-Based CO2 Capture System using Pilot Plant Data, 11th IFAC Symposium on Dynamics and Control of Process Systems, including Biosystems, (2016).
[67] N. Ceccarelli, M. van Leeuwen, T. Wolf, P. van Leeuwen, R. van der Vaart, W. Maas, A. Ramos, Flexibility of Low-CO2 Gas Power Plants: Integration of the CO2 Capture Unit with CCGT Operation, Energy Procedia, 63 (2014) 1703-1726.